NASA/CR—2001-210685 AIAA–2001–0233

# Aero-Thermal Calibration of the NASA Glenn Icing Research Tunnel (2000 Tests)

Jose C. Gonsalez, E. Allen Arrington, and Monroe R. Curry III
Dynacs Engineering Company, Inc., Brook Park, Ohio

Prepared for the
39th Aerospace Sciences Meeting and Exhibit
sponsored by the American Institute of Aeronautics and Astronautics
Reno, Nevada, January 8–11, 2001

Prepared under Contract NAS3–98008

National Aeronautics and
Space Administration

Glenn Research Center

March 2001

Available from

NASA Center for Aerospace Information
7121 Standard Drive
Hanover, MD 21076
Price Code: A03

National Technical Information Service
5285 Port Royal Road
Springfield, VA 22100
Price Code: A03

Available electronically at http://gltrs.grc.nasa.gov/GLTRS

# AERO-THERMAL CALIBRATION OF THE NASA GLENN ICING RESERCH TUNNEL (2000 TESTS)

Jose C. Gonsalez,* E. Allen Arrington,† and Monroe R. Curry III‡
Dynacs Engineering Company, Inc.
Brook Park, Ohio 44142

## Abstract

Aero-thermal calibration measurements and flow quality surveys were made in the test section of the Icing Research Tunnel at the NASA Glenn Research Center. These surveys were made following major facility modifications including widening of the heat exchanger tunnel section, replacement of the heat exchanger, installation of new turning vanes, and installation of new fan exit guide vanes. Standard practice at NASA Glenn requires that test section calibration and flow quality surveys be performed following such major facility modifications. A single horizontally oriented rake was used to survey the flow field at several vertical positions within a single cross-sectional plane of the test section. These surveys provided a detailed mapping of the total and static pressure, total temperature, Mach number, velocity, flow angle and turbulence intensity. Data were acquired over the entire velocity and total temperature range of the facility. No icing conditions were tested; however, the effects of air sprayed through the water injecting spray bars were assessed. All data indicate good flow quality. Mach number standard deviations were less than 0.0017, flow angle standard deviations were between 0.3 and 0.8 degrees, total temperature standard deviations were between 0.5 and 1.8 °F for sub-freezing conditions, axial turbulence intensities varied between 0.3 and 1.0%, and transverse turbulence intensities varied between 0.3 and 1.5%. Measurement uncertainties were also quantified.

## Nomenclature

| | |
|---|---|
| $a, b, c$ | Hot wire curve fit coefficients |
| $C_\alpha$ | Pitch angle pressure coefficient |
| $C_\beta$ | Yaw angle pressure coefficient |
| $C_o$ | Total pressure coefficient |
| $C_q$ | Static pressure coefficient |
| $C_t$ | Total temperature recovery coefficient |
| $E$ | Hot wire anemometer output voltage, volts |
| $H$ | Test section height, 72-inches |
| $K_0$ to $K_2$ | Flow angle prediction coefficients, degrees |
| $N$ | Number of data points |
| $M$ | Mach number |
| $P$ | Pressure, psia |
| $P_{air}$ | Spray bar air pressure, psig |
| $P_1$ to $P_9$ | Flow angle probe pressures, psia |
| $P_{1\text{-}4,avg}$ | Average of $P_1$, $P_2$, $P_3$, and $P_4$, psia |
| $P_{6\text{-}9,avg}$ | Average of $P_6$, $P_7$, $P_8$, and $P_9$, psia |
| $q$ | Dynamic pressure, psi |
| $R$ | Specific gas constant for air, 1716 $ft^2/(sec^2\ °R)$ |
| $T$ | Temperature, °F display, °R calculations |
| $T_{D,avg}$ | Average of the twenty-four Corner D total temperature measurements, °F |
| $TI_u$ | Axial turbulence intensity, % |
| $TI_v$ | Transverse turbulence intensity, % |
| $u$ | Hot wire axial velocity, ft/sec |
| $v$ | Hot wire transverse velocity, ft/sec |
| $V$ | Velocity, ft/sec, mph, or knots |
| $W$ | Test section width, 108-inches |
| $X$ | Axial coordinate with axis origin at bellmouth/test section weld seam, inches |
| $Y$ | Spanwise coordinate with axis origin at the test section inner wall, inches |
| $Z$ | Vertical coordinate with axis origin at the test section floor, inches |
| $\alpha$ | Pitch flow angle, degrees |
| $\beta$ | Yaw flow angle, degrees |
| $\Delta$ | Measured pitch or yaw angle offset, degrees |
| $\gamma$ | Ratio of specific heats, 1.4 |
| $\sigma$ | Standard deviation |
| $\theta$ | Hot wire sensor inclination angle, degrees |

*Subscripts*

| | |
|---|---|
| *avg* | Average |
| *bellmouth* | Pertaining to the pitot-static probes at the bellmouth exit / test section inlet |
| *eff* | Pertaining to hot wire effective velocities |
| *Faro* | Pertaining to the 6 degree-of-freedom digitizing arm |
| *HW* | Pertaining to a hot wire probe |
| *i* | Data point index or hot wire sensor index |

*Aerospace Engineer
†Aerospace Engineer, Senior Member AIAA
‡Mechanical Engineer

| | |
|---|---|
| *level* | Pertaining to a digital level |
| *local* | Pertaining to parameters in the test section after all probe calibration coefficients have been taken into account |
| *optical* | Pertaining to an optical transit |
| *rake* | Pertaining to the 9-foot survey rake |
| *ruler* | Pertaining to a tape measure or ruler |
| *S* | Static conditions |
| *T* | Total or stagnation conditions |
| $\alpha$ | Pertaining to pitch angle |
| $\beta$ | Pertaining to yaw angle |

## Introduction

As part of the continuing efforts to upgrade and improve the test facilities at the NASA Glenn Research Center, Cleveland, Ohio, several major modifications were made to the Icing Research Tunnel (IRT). These modifications were aimed at improving icing and aero-thermal characteristics as well as improving the operational efficiency of the facility. Since these modifications were extensive and affected several key components of the tunnel, a comprehensive implementation and recommissioning plan was developed and executed to insure success.

The most significant modification was the replacement of the wind tunnel heat exchanger. The original heat exchanger was a folded or W-shaped configuration, which provided maximum cooling area. While very effective in producing the low temperatures needed for icing conditions, the folded design had a negative impact on the aerodynamic flow quality. This, coupled with the fact that the aging heat exchanger was becoming increasingly difficult to maintain, lead to the decision to replace the folded heat exchanger with a flat heat exchanger.[1] This required the demolition of about a quarter of the tunnel loop and subsequent widening of the tunnel shell to accept the larger flat heat exchanger. New corner turning vanes were installed upstream and downstream of the heat exchanger to insure an even distribution of airflow into and out of the heat exchanger leg.

A second major modification that impacted the tunnel flow quality was the installation of exit guide vanes (EGVs) immediately downstream of the facility drive fan. The EGVs were designed to produce a more even flow field downstream of the fan. Previous tests (Reference 1) indicated several flow quality concerns in the area downstream of the drive system, which were thought to be caused by the blockage of the drive motor housing support legs. The EGVs were designed to keep the flow exiting the fan more evenly distributed around the drive motor housing, thereby resulting in improved flow quality entering the heat exchanger leg. More information about the IRT facility modifications can be found in Reference 2.

As part of the IRT recommissioning activities, loop flow quality, test section aero-thermal calibration/flow quality, and icing cloud calibration measurements were conducted. The loop flow quality measurements were carried out in January 2000 and are documented in Reference 3. The icing cloud calibration measurements (liquid water content and droplet size) were made in early 2000 and are documented in Reference 4. Baseline test section calibration and flow quality measurements were made in April 1997 prior to the facility modifications and the results of these measurements can be found in Reference 5. Test section calibration and flow quality measurements following the facility modifications were carried out in April 2000. The focus of this paper will be these results from this test program and the comparison of these results to those from 1997.

NASA Glenn has a policy of maintaining up-to-date calibration and flow quality information about each of its large wind tunnels. NASA Glenn has implemented a plan to perform full test section calibrations and flow quality measurements every two to three years and to perform check calibrations one to two times per year in every one of its major wind tunnel facilities. Full test section calibrations are also performed every time major facility modifications are carried out. Data collected from these tests are assembled into a database and checked to insure that the facility is in statistical quality control.

IRT test section calibration and flow quality measurements were obtained using a custom built 9-foot horizontal survey rake. The rake measured total pressure, static pressure, total temperature, flow angle, and turbulence intensity at a single cross-sectional plane in the test section. Data from this rake were used to construct calibration curves for the tunnel pitot-static probes at the test section inlet and the tunnel total temperature probes in the settling chamber. The data were also used to assess the general flow quality of the test section. The objectives of this paper are given below:

1. Briefly describe the Icing Research Tunnel (before and after major facility modifications) and the test hardware and facility instrumentation used during this test program.

[1]Actually, two flat exchangers were installed nearly side by side in the expanded tunnel loop. These two flat heat exchangers provided the same amount of cooling capacity of the original folded design, without the inherent degradation of flow quality. For simplicity, these two heat exchangers will be referred to as the heat exchanger.

2. Describe the test procedures and the test matrix used to carry out the test program.
3. Describe the data reduction procedures.
4. Present total pressure recoveries, static pressure recoveries, Mach number recoveries, total temperature recoveries, flow angles, and turbulence intensities at a single cross-sectional plane in the test section.
5. Present data describing the effects of air sprayed through the water injecting spray bars on test section aerodynamic properties and flow quality.
6. Present calibration curves that correlate the total pressure, static pressure, dynamic pressure, velocity, and total temperature at a single cross-sectional plane in the test section to the total and static pressure measured by the pitot-static probes at the test section inlet and to the total temperature measured by probes on the corner D turning vanes.
7. Quantify the uncertainties in the measured and calculated data.
8. Where appropriate, directly compare the 2000 results to the 1997 results.

## Icing Research Tunnel Description

The NASA Glenn Icing Research Tunnel is a closed-loop atmospheric tunnel with rectangular cross sections. The airflow is driven by a 25-foot diameter twelve blade fan that is powered by a 5000-horsepower electric motor. The tunnel test section is 6-feet high, 9-feet wide, and 20-feet long. There is no divergence along any of the test section surfaces. The velocity in an empty test section can be varied between 50 and 390 mph (Mach numbers between 0.065 and 0.56) at 0 °F. A set of ten horizontally oriented spray bars, located in the settling chamber at the bellmouth inlet, inject atomized water into the airflow to create icing conditions. The tunnel has been in service since 1944 and has undergone several major upgrades and modifications over the years to insure that it remains the premiere ground test facility for icing research. As previously mentioned, the tunnel was recently modified by replacing the original folded heat exchanger with two adjacent flat heat exchangers to improve both the aerodynamic flow quality and the icing cloud characteristics. To accommodate the new heat exchanger, the C-D leg of the tunnel loop was expanded. This tunnel expansion required new turning vanes to be installed in C and D corners. The C corner tuning vanes were designed to turn and expand the flow into the larger heat exchanger section. The D corner vanes were designed to turn and contract the flow into the smaller settling chamber area. Exit guide vanes were also installed downstream of the fan to improve the flow quality entering the heat exchanger. Figure 1 shows the IRT planview as it was in April of 1997 prior to the heat exchanger replacement. Figure 2 shows the IRT planview as it is now with the C-D leg widened, with the new flat heat exchanger, with new C and D corner turning vanes, and with new fan outlet guide vanes. Figure 3 is an elevation schematic view of the old IRT folded "W" heat exchanger. Figure 4 is a photograph of the new IRT flat exchanger. It can be seen how the flat heat exchanger is actually composed of two smaller heat exchangers positioned side by side. It can be seen in Figure 2 that aerodynamic fairings are used to smoothly transition the flow over the heat exchanger discontinuity. More information about the IRT facility can be found in Reference 6.

## Test Hardware and Facility Instrumentation

### Test Section (9-foot) Survey Rake

Figure 5 is a photograph of the 9-foot horizontal survey rake installed in the IRT test section at a vertical height of $Z$=36-inches (centerline). This rake is the primary tool for carrying out full test section calibrations and flow quality measurements. Figure 6 shows an exploded planview of the IRT test section with the survey rake installed. The rake was installed at an axial position of $X$=179.3-inches which was the axial station of the cross-sectional plane surveyed during this test program as well as the test program in 1997. Figure 7 shows the plan and front views of the survey rake. Figure 8 shows a cross-section of the survey rake and has exploded views of the flow angle pressure probe ports. Note that the origin of the $X$-$Y$-$Z$ coordinate system is as follows: the $X$ axis origin is at the bellmouth/test section weld seam as seen in Figure 6, the $Y$ axis origin is at the inner wall as seen in Figure 6, and the $Z$ axis origin is at the floor as seen in Figure 5.

The instrumentation mounted on the 9-foot survey rake includes eleven flow angle pressure probes, eleven total temperature thermocouple probes, and three single sensor or dual sensor hot wire probes. The spanwise, $Y$ positions of all probes with respect to the test section inner wall are defined in Figure 7. The survey rake was supported at both ends by bolting the rake to wall mounted support plates as seen in Figure 5. These support plates are 6-feet tall and have a bolt pattern that allow the rake to be positioned vertically every 6-inches above or below the test section centerline. A vertical strut, shown in Figure 5, was also used to support the rake in the center. As seen in Figure 8, the main body of the rake is formed by two aluminum I-beams and thin aluminum plates riveted together. Thin sheets of aluminum were bent to form the leading and trailing edge of the rake body.

The flow angle pressure probes are bolted to the rake body I-beams as seen in Figure 8. These probes are of

hemi-spherical head design and have five total pressure ports in the head. The four circumferential total pressure ports measure pitch and yaw angle. The center port measures total pressure. Four static pressure ports are located downstream of the head. Details of these pressure ports can be seen in Figure 8. The heads of the probes are 20.75-inches upstream of the rake leading edge. The static pressure taps on each probe are 5.75-inches downstream of the head. The probes were calibrated for Mach numbers between 0.1 and 0.6 in the NASA Glenn 3.5-inch diameter free jet calibration facility. Details of the probe calibration can be found in Reference 7.

Aspirated total temperature thermocouple probes with copper/constantan (type T) wires were used. These probes are depicted in Figures 5, 7, and 8. The probes are mounted to the bottom surface of the survey rake with the tips of the probes about 0.5-inches upstream of the rake leading edge and 2.0-inches below the rake centerline. The total temperature probes were calibrated for total temperature recovery in the NASA Glenn 3.5-inch diameter free jet calibration facility.

Three single sensor or dual sensor hot wire probes (0.00015-inch diameter tungsten wires) were used. The probes were mounted to the upper surface of the rake body as depicted in Figures 5, 7, and 8. The probe tips were located 9.75 inches upstream of the rake body leading edge and 3.0-inches above centerline.

Facility Instrumentation

The following standard facility instrumentation was used during this test program:

1. Bellmouth/test section pitot-static probes: Two probes are mounted at the test section inlet, just downstream of the bellmouth, one on the inner wall and one on the outer wall. These probes are used to measure the test section total and static pressure. Measurements from both probes are averaged to arrive at $P_{T,bellmouth}$ and $P_{S,bellmouth}$. These probes are shown in Figure 6.
2. Total temperature probes in corner D: Twenty-four total temperature type "T" thermocouple probes are arrayed on the turning vanes in corner D to measure the temperature profile exiting the facility cooler. The average of these twenty-four probes is used as the test section total temperature, $T_{D,avg}$. The approximate locations of these probes are shown in Figure 2. Prior to the 1999 facility modifications, eleven total temperature probes were used in Corner D. The number was increased to twenty-four following the installation of the new heat exchanger.

Steady-State Data Acquisition System

Real-time steady-state data acquisition and data display was provided by a NASA Glenn Escort Alpha system. This system is the standard data acquisition and data display system used in the large test facilities at NASA Glenn. The system accommodates inputs from the Electronically Scanned Pressure System (ESP), inputs from the facility distributed process control system, and inputs from any analog devices such as thermocouples and pressure transducers. This system recorded all steady-state pressures and temperatures from the 9-foot survey rake, the tunnel bellmouth pitot-static probes, and the total temperature probes in Corner D. It also recorded important facility parameters such as fan rotational speed and spray bar air pressure.

The Electronically Scanned Pressure system used during this test program utilized plug-in modules that each contained 32 individual transducers with individual ports. Each transducer/port can be addressed separately and scanned at a rate of 10,000 ports per second. Calibration of all ESP transducers was performed automatically by the system at least every 30 minutes. For this test program, $\pm$5 psid modules were used.

Hot Wire Instrumentation

Commercially available constant temperature anemometers were used for the hot wire turbulence intensity measurements. Three anemometers were used for the three single sensor hot wire probes and six were required for the three dual sensor hot wire X probes. Each anemometer was equipped with its own signal conditioner for low-pass filtering, DC offsetting, and amplifying. Commercially available 12-bit personal computer based analog-to-digital converter data acquisition boards were used to digitize the hot wire signals. These boards had multiple input voltage ranges so that an optimal input range could be selected. This range was generally $\pm$5 volts. A commercially available personal computer based graphical programming software package was used to build a customized hot wire data acquisition program with graphical user interface, data reduction/processing, and data archiving capabilities. This customized hot wire system was linked to the facility Escort computer so that data acquisition could be synchronously acquired with one trigger.

The hot wire probes were not calibrated prior to the test. They were calibrated in place using the velocities measured by the 5-hole flow angle pitot-static pressure probes. Data were acquired at small enough velocity increments to be able to generate calibration curves for

the hot wires. The probes were generally used from 50 mph to 250 mph. The hot wires generally broke at speeds above 250 mph. Over this speed range, the raw unconditioned bridge output voltages varied between 1.3 and 1.8 Volts.

## Test Matrix and Test Procedures

Table 1 shows the test matrix for the IRT April 2000 test section calibration program with the 9-foot horizontal survey rake. As previously indicated, all measurements were carried out at an axial station of $X$=179.3-inches. For the 9-foot horizontal rake, data were acquired at eleven elevations, at multiple temperatures between 70 (ambient) and -20 °F, and for test section velocities up to 350 mph. For every elevation, the tunnel had to be stopped and the rake had to be moved manually. At the $Z$=36-inch elevation and for temperatures of 70 and 40 °F, data were acquired with ($P_{air}$ = 80 psig) and without ($P_{air}$ = 0 psig) air being sprayed through the water injecting spray bars. This was done to assess the effects of air spray on test section flow quality. Hot wire data were acquired for test section velocities less than or equal to 250 mph and for 70 and 40 °F temperatures. Pressure data were taken for 70 and 40 °F temperature only. For freezing and sub-freezing temperatures, ice would form on the pressure probes and invalidate the pressure data. For this reason, covers were installed on the 5-hole flow angle pitot-static pressure probes for freezing and sub-freezing temperatures to minimize the infiltration of ice and water into the pressure ports.

A number of additional testing procedures are noteworthy. On a few occasions, a number of the pressure ports on the 5-hole probes had to be purged to eliminate moisture. At 40 °F and at higher test section speeds, a significant amount of water would condense in the air and plug the pressure ports on the 5-hole probes. It was evident during data acquisition that some data would have to be discarded due to this problem. When hot wire data was being acquired the tunnel would be run up to 250 mph and then either shut down or brought down to a fan idle condition so that the hot wire probes could be removed. The hot wire probes just would not survive above 250 mph. When temperature data were being acquired at sub-freezing conditions, the tunnel would have to be stopped or brought to an idle fan condition so that ice could be removed from the total temperature probes. Even though no water was being injected into the tunnel, the thermal and velocity cycling of the tunnel tended to bring in a significant amount of moisture from the atmosphere. In addition, the tunnel did not have a chance to dry out with testing going on 5 days a week for about 8 to 12 hours at a time.

For each configuration in the test matrix, steady state pressure, temperature, and facility data were collected over the test section velocity range using the IRT Escort Alpha system. When hot wire data were being acquired, a single trigger captured both steady state Escort data and hot wire data. For each point in the test matrix, three data readings were recorded. Each steady state Escort reading was the average of 15 single scans (15 seconds) of data. Ten seconds of hot wire data were collected for every reading. In general, the slowest airspeed conditions were tested first. Wind-off readings were recorded prior to and following each tunnel run. Table 2 is a listing of typical test conditions recorded during this April 2000 test program.

Prior to the first tunnel run, the flow angle probe pitch and yaw offset angles were measured with respect to the tunnel centerline using a six-degree of freedom digitizing arm. Along with these measurements, separate more easily obtained pitch and yaw offset angles were obtained with a digital level and a tape measure or ruler. The combination of these measurements formed the baseline pitch and yaw offset angles. For each vertical rake height change (a change in $Z$), the flow angle probe pitch and yaw offset angles were measured again with the digital level and a tape measure and compared to the baseline values. All changes from the baseline were recorded and were later used to correct the pitch and yaw angles generated by the data reduction process.

Every time hot wire data were recorded, they were recorded for all three probes simultaneously by individual analog-to-digital converter data acquisition boards residing in a personal computer. The data acquisition boards were configured to sample either three or six channels simultaneously (depending on whether single sensor or dual sensor X probes were used) at a rate of 10000 samples per second and to acquire 100000 data points per channel. This worked out to be 10 seconds of data for each channel. The signal conditioners for each hot wire probe were configured to low pass filter at 4000 Hz, to DC offset with –1 volt, and to amplify with a gain of 5.

## Data Reduction

Data reduction can basically be divided up into five groups: (1) pressure, (2) temperature, (3) velocity, (4) flow angle, and (5) turbulence intensity. Each group will be visited briefly. It is important to understand that the subscript "*bellmouth*" refers to parameters (measured or calculated) associated with the two bellmouth pitot-static probes located on the inner and outer test section walls (at the bellmouth exit or test section inlet, see Figure 6). The subscript "*rake*" refers

to parameters (measured or calculated) associated with any of the probes on the 9-foot survey rake. The subscript "*local*" refers to the same parameters as the "*rake*" parameters except that the "*local*" parameters have been corrected by individual probe calibration coefficients and represent the true "*local*" properties in the test section. Note that all "*local*" total pressures, static pressures, and Mach numbers are normalized by "*bellmouth*" parameters to arrive at recovery ratios. All of the compressible flow equations used in the data reduction can be found in Reference 8.

Pressure

The following equations were used to reduce the pressure data and apply to all eleven individual 5-hole flow angle pitot-static pressure probes.

$$P_{6-9,avg} = \frac{\left(P_6 + P_7 + P_8 + P_9\right)}{4}$$

$$M_{rake} = \sqrt{\frac{2}{\lambda - 1}\left[\left(\frac{P_5}{P_{6-9,avg}}\right)^{\frac{\gamma-1}{\gamma}} - 1\right]}$$

$$P_{T,local} = P_5 - C_o\left(M_{rake}\right)\cdot\left[P_5 - P_{6-9,avg}\right]$$

$$P_{S,local} = P_{T,local} - \frac{\left(P_5 - P_{6-9,avg}\right)}{C_q\left(M_{rake}\right)}$$

$$M_{local} = \sqrt{\frac{2}{\lambda - 1}\left[\left(\frac{P_{T,local}}{P_{S,local}}\right)^{\frac{\gamma-1}{\gamma}} - 1\right]}$$

$$M_{bellmouth} = \sqrt{\frac{2}{\lambda - 1}\left[\left(\frac{P_{T,bellmouth}}{P_{S,bellmouth}}\right)^{\frac{\gamma-1}{\gamma}} - 1\right]}$$

$$q_{local} = \frac{\gamma}{2}\cdot M_{local}^2 \cdot P_{S,local}$$

$$q_{bellmouth} = \frac{\gamma}{2}\cdot M_{bellmouth}^2 \cdot P_{S,bellmouth}$$

$C_o$ and $C_q$ are functions of $M_{rake}$ and were experimentally determined when the flow angle pressure probes were calibrated. Values for these coefficients can be found in Reference 7. $\gamma$ is the ratio of specific heats for air and is equal to 1.4. Pressures $P_5$ through $P_9$ are measured directly from the flow angle pressure probes.

Temperature

The following equations were used to reduce the temperature data. The equations containing "*local*" and "*rake*" parameters apply to all eleven individual total temperature probes.

$$T_{T,local} = C_t\left(M_{local}\right)\cdot T_{rake}$$

$$T_{S,local} = T_{T,local}\cdot\left(1 + \frac{\gamma - 1}{2}M_{local}^2\right)^{-1}$$

$$T_{T,bellmouth} = T_{D,avg} = \frac{1}{24}\sum_{i=1}^{24} T_{D,i}$$

$$T_{S,bellmouth} = T_{T,bellmouth}\cdot\left(1 + \frac{\gamma - 1}{2}M_{bellmouth}^2\right)^{-1}$$

$C_t$ is the recovery coefficient for each individual total temperature probe and is a function of $M_{local}$. These coefficients were determined experimentally when the probes were calibrated in the NASA Glenn 3.5-inch diameter free jet calibration facility. The total temperature probes gradually predict temperatures lower than the actual temperature as the local Mach number increases. At a local Mach number of 0.1, typical values of $C_t$ are 1.001 and at a local Mach number of 0.6, the values of $C_t$ are generally around 1.005. At the time this paper was written, the values of $C_t$ had not been documented in a formal report. Note that all of the temperatures presented in this paper are in °F, but all calculations were carried out in °R including the total temperature recovery ratios.

Velocity

Velocities were calculated using the equations presented in this section. Equations containing "*local*" parameters apply to all eleven individual flow angle pressure probes.

$$V_{local} = M_{local}\cdot\sqrt{\gamma R T_{S,local}}$$

$$V_{bellmouth} = M_{bellmouth}\cdot\sqrt{\gamma R T_{S,bellmouth}}$$

$R$ is the specific gas constant for air and is equal to 1716 $ft^2$ / ($sec^2$ °R).

Flow Angle

The equations in this section were used to generate pitch and yaw flow angle data from the raw pressure data obtained from the flow angle pressure probes.

$$P_{1-4,avg} = \frac{P_1 + P_2 + P_3 + P_4}{4}$$

$$C_\alpha = \frac{(P_3 - P_1)}{(P_5 - P_{1-4,avg})}$$

$$C_\beta = \frac{(P_4 - P_2)}{(P_5 - P_{1-4,avg})}$$

$$\alpha = K_{0,\alpha}(M_{rake}) + K_{1,\alpha}(M_{rake}) \cdot C_\alpha + \Delta_{\alpha,Faro} + \Delta_{\alpha,level}$$

$$\beta = K_{0,\beta}(M_{rake}) + K_{2,\beta}(M_{rake}) \cdot C_\beta + \Delta_{\beta,Faro} + \Delta_{\beta,ruler}$$

Pressures $P_1$ through $P_5$ are measured directly from the flow angle pressure probes. The coefficients $K_{0,\alpha}$, $K_{1,\alpha}$, $K_{0,\beta}$, and $K_{2,\beta}$ are all functions of $M_{rake}$ and were experimentally determined when the flow angle pressure probes were calibrated in the NASA Glenn 3.5-inch diameter free jet calibration facility. Values for these coefficients are documented in Reference 7. The $\Delta_{\alpha,Faro}$ and $\Delta_{\beta,Faro}$ values were constant for every $Z$ elevation and were determined by measuring the pitch and yaw offset angles for the probes with a six degree of freedom digitizing arm. The $\Delta_{\alpha,level}$ and $\Delta_{\beta,ruler}$ values were different for every $Z$ elevation but were equal to 0 degrees for the $Z$=36-inch elevation since it was at this elevations that the baseline measurements were taken. These values were determined by taking measurements with a digital level and a ruler and comparing these measurements to the baseline values. Deviations from the baseline numbers were entered as $\Delta_{\alpha,level}$ and $\Delta_{\beta,ruler}$.

Turbulence Intensity

As was previously indicated, the hot wire probes were not calibrated prior to use in the IRT. The significantly varying temperatures and static pressures associated with testing in the IRT make it very difficult to build accurate calibration curves in a separate calibration facility. For this reason, in-situ calibration of the hot wire probes was performed. Data were acquired in such a way that calibration curves could be constructed after the data were acquired. After acquisition, the hot wire data were reduced so that average bridge voltages were available for every probe sensor and for every test condition. These data points were matched up with air velocities from the flow angle pressure probes on the 9-foot survey rake for the same test conditions. Calibration curves (exponential functions with effective air velocity as a function of hot wire bridge voltage) were generated for each hot wire probe sensor. The equations used in this curve-fit process are given below.

$$V_{HW,eff,i} = V_{local} \cdot \cos\theta_{HW,i}$$

$$V_{HW,eff,i} = a_i \cdot E_{HW,i} + b_i \cdot e^{c_i \cdot E_{HW,i}}$$

where $i$ = 1 to 1 for a single sensor hot wire probe
and $i$ = 1 to 2 for a dual sensor hot wire X probe.

$\theta_{HW,i}$ is the angle of the hot wire sensor relative to the freestream velocity vector minus 90°. For a single sensor probe, the sensor is normal to the velocity vector and $\theta_{HW,1}$ is (90° – 90° =) 0° for this case. For a dual sensor X probe at 0° angle of attack, one sensor is at 45° and the other is at 135° relative to the velocity vector. For these two sensors, $\theta_{HW,1}$ is (45° – 90° =) –45° and $\theta_{HW,2}$ is (135° – 90° =) +45°. Once the values of $V_{HW,eff,i}$ are computed, these values along with the corresponding values of hot wire anemometer bridge voltage, $E_{HW,i}$ can be used to arrive at values of $a_i$, $b_i$, and $c_i$ via non-linear least squares curve-fitting using the exponential equation given above.

The reader may be wondering how accurate flow angles and transverse velocities can be computed by the dual sensor X probe if no angular calibration data are used. To answer this question, two key assumptions are called upon. The first key assumption is that the X probes will only be used to assess the unsteadiness in flow angle and will not be used to quantify the absolute flow angle. The resulting flow angles and transverse velocities will all be centered around zero and have averages essentially at zero. This should work fine in the IRT test section since we know that the flow angles will be small (typically ±2° or less) and will be centered about zero. The second key assumption is that the X probes used in this test behave like other X probes previously calibrated through various flow angles. The results for an X probe calibrated through various flow angles show that the calibration map will collapse down to one curve

when effective velocity is plotted versus hot wire anemometer bridge voltage. This is typically true for angles between ±20°.

Given the exponential curve fit equation used to relate hot wire effective velocity to hot wire anemometer bridge voltage, hot wire data reduction can continue with the equations given below for a dual sensor hot wire X probe.

$$V_{HW} = \sqrt{V_{HW,eff,1}^2 + V_{HW,eff,2}^2}$$

$$\alpha_{HW} = 45^\circ - \tan^{-1}\left(\frac{V_{HW,eff,2}}{V_{HW,eff,1}}\right)$$

$$u_{HW} = V_{HW} \cdot \cos(\alpha_{HW})$$

$$v_{HW} = V_{HW} \cdot \sin(\alpha_{HW})$$

For a single sensor hot wire probe, the following equalities are used instead of the four equations above.

$$u_{HW} = V_{HW} = V_{HW,eff,1}$$

Once $u_{HW}$ is available for a single sensor probe, and $u_{HW}$ and $v_{HW}$ are available for dual sensor X probe, statistics necessary for computing turbulence intensity can be calculated using the equations given below. The value of N used was 100000.

$$u_{HW,avg} = \frac{1}{N}\sum_{i=1}^{N} u_{HW,i}$$

$$v_{HW,avg} = \frac{1}{N}\sum_{i=1}^{N} v_{HW,i}$$

$$V_{HW,avg} = \sqrt{u_{HW,avg}^2 + v_{HW,avg}^2}$$

$$\sigma_{u_{HW}} = \sqrt{\frac{1}{N-1}\sum_{i=1}^{N}\left(u_{HW,i} - u_{HW,avg}\right)^2}$$

$$\sigma_{v_{HW}} = \sqrt{\frac{1}{N-1}\sum_{i=1}^{N}\left(v_{HW,i} - v_{HW,avg}\right)^2}$$

$$TI_u = \frac{\sigma_{u_{HW}}}{V_{HW,avg}} \times 100\%$$

$$TI_v = \frac{\sigma_{v_{HW}}}{V_{HW,avg}} \times 100\%$$

Since in-situ calibration curves were generated, there was no need to correct for changes in temperature or static pressure. The calibration curves took care of these inherent variations. In addition, new calibration curves were generated for every velocity sweep. More information about hot wire anemometry can be found in Reference 9.

## Discussion of Results

Flow quality results for the single cross-sectional plane surveyed ($X$=179.3-inches) will be presented in terms of total pressure, static pressure, Mach number, flow angle, total temperature, and turbulence intensity. Results describing the effects of air sprayed through the water injecting spray bars will also be presented. Results will be compared to 1997 results. Calibration curves for total pressure, static pressure, dynamic pressure, velocity, and total temperature will also be defined. Finally, uncertainties for key parameters will be reported. Where appropriate, local test section data were normalized by bellmouth parameters to account for any run-to-run variations. To put the flow quality results into perspective, comparisons will be made to the NASA Glenn flow quality goals for the Icing Research Tunnel.

### Flow Quality Goals

Specific aerodynamic flow quality goals for the Icing Research Tunnel were developed based on input from the 1989 Wind Tunnel Calibration Workshop held at the NASA Langley Research Center and from IRT research customer requirements. The goals reflect the general mission of the IRT and are listed below:

1. The Mach number range should be less than or equal to 0.005 (0.00083 in terms of standard deviation).
2. The flow angle range should be less than or equal to 0.5 degrees (0.083 degrees in terms of standard deviation).
3. Turbulence intensity should be less than or equal to 0.5%.
4. The total temperature range should be less than or equal to 2 °F (0.33 °F in terms of standard deviation).

The standard deviation numbers are one-sixth of the range values. If the parameter distributions are assumed to be normal, then six standard deviations (or the range) will essentially provide 100% coverage.

Statistical Flow Quality Results

Before graphical results are presented, an introduction to Table 3 will be helpful. Table 3 contains statistical flow quality results for all parameters and the corresponding flow quality goals for comparison. Results are presented for the single cross-sectional plane surveyed ($X$=179.3-inches) and for test section velocities of 100, 200, and 300 mph. In addition, results are presented for the full 6×9-foot cross-section and for a reduced 4×5-foot centered cross-section.

Total Pressure

Figure 9 shows the total pressure recovery in the test section for velocities of 100, 200, and 300 mph. The total pressure surfaces are generally flat with only minor deviations. From Table 3, the 6×9-foot total pressure ranges are 0.003, 0.030, and 0.030 psi (standard deviation are 0.00053, 0.00303, and 0.00312 psi) respectively for the three velocities. For the 4×5-foot cross-section, the ranges are 0.002, 0.021, and 0.025 psi (standard deviations are 0.00052, 0.00191, and 0.00295 psi) respectively.

Static Pressure

Figure 10 shows the static pressure recovery in the test section for velocities of 100, 200, and 300 mph. The static pressure surfaces generally develop a more pronounced rectangular "bowl" shape with increasing velocity. From Table 3, the 6×9-foot static pressure ranges are 0.006, 0.024, and 0.048 psi (standard deviations are 0.00131, 0.00492, and 0.01026 psi) respectively for the three velocities. For the 4×5-foot cross-section, the ranges are 0.004, 0.014, and 0.036 psi (standard deviations are 0.00081, 0.00299, and 0.00669 psi) respectively.

Mach number

Figure 11 shows the Mach number recovery in the test section for velocities of 100, 200, and 300 mph. The Mach number surfaces generally drop-off as the test section walls are approached. From Table 3, the 6×9-foot Mach number ranges are 0.003, 0.005, and 0.006 (standard deviations are 0.00053, 0.00095, and 0.00139) respectively for the three velocities. For the 4×5-foot cross-section, the ranges are 0.001, 0.004, and 0.005 (standard deviations are 0.00030, 0.00062, and 0.00090) respectively for the three velocities. The IRT test section (for the 4×5-foot area) essentially meets the Mach number range goal of 0.005 and the standard deviation goal of 0.00083 for test section velocities less than 300 mph.

Flow Angles

Figure 12 shows the flow angle vectors in the test section for velocities of 100, 200, and 300 mph. The vectors represent the resultant of the pitch and yaw angles sensed by the flow angle pressure probes. The length of the vector represents the magnitude of the resultant and the orientation provides the direction of the flow. It should be noted that vectors for $Y$=9 and 18-inches appear to be biased toward the test section ceiling. The pressure data as well as the probe alignment angles were scrutinized. There was no evidence of systematic or random errors above and beyond the normal instrumentation and alignment uncertainties. The flow angles appear to be well behaved except for the upflow near the inner wall. Some small areas of circulation may be evident; however, they are not well defined.

From Table 3, the 6×9-foot pitch angle ranges are 2.97, 3.94, and 3.16 degrees (standard deviations are 0.588, 0.653, and 0.648) respectively for the three velocities. The yaw angle ranges are 2.40, 2.51, and 1.96 degrees (standard deviations are 0.364, 0.404, and 0.336) respectively. For the 4×5-foot cross-section, the pitch angle ranges are 2.05, 2.11, and 2.07 degrees (standard deviations are 0.380, 0.409, and 0.424) respectively for the three velocities. The yaw angle ranges are 1.70, 2.51, and 1.82 degrees (standard deviations are 0.323, 0.412, and 0.327) respectively. The IRT test section does not meet the flow angle range goal of 0.5 degrees (or the standard deviation goal of 0.083 degrees). It can be seen in Table 3, that the average of all flow angles for all cross-sections is between –0.25 and +0.21 degrees. This is good considering the large ranges. In addition, the IRT does not have any flow straightening devices in the settling chamber. Honeycomb would certainly reduce the flow angle variation.

In general, the flow angles indicate that no significant problems with flow direction were introduced with the heat exchanger replacement and the installation of the Corner D turning vanes.

Total Temperature

Figure 13 shows the total temperature recovery in the test section for velocities of 150, 250, and 350 mph and for a tunnel total temperature of $T_{D,avg}$ = 30 °F. Figure 14 shows the same data for of $T_{D,avg}$ = 0 °F. From the surfaces, it appears that there is more vertical variation and than spanwise variation. This is a result of the data acquisition technique. Data were collected in spanwise

profiles and data at different vertical positions were not taken at the same time. The test section temperature distribution has some variability with time, so the vertical variability has more to do with time variation than spatial variation.

Figure 15 shows total temperature recovery profiles on centerline ($Z$=34-inches) for three different air speeds (100, 200, and 300 mph), for the years 1997 and 2000, and for a number of different temperatures ranging between 40 and –20 °F. It is apparent from these graphs that the spanwise temperature profile variability has been reduced with the new flat heat exchanger.

An extensive amount of temperature data were obtained in the year 2000 following the heat exchanger replacement. The statistical results from these temperature measurements are summarized in Table 4. Shown in Table 4 are statistical results for the full 6×9-foot area and the smaller 4×5-foot area in terms of maximum, minimum, range, average, and standard deviation. Results are reported for test section airspeeds of 50, 150, 250, and 350 mph and for temperatures around ambient, 40, 30, 0, and –20 °F. The NASA Glenn IRT temperature variation goals are also shown (2.0°F for range and 0.33°F for standard deviation). For the 6×9-foot area, the minimum range is 4.86 °F with a standard deviation of 0.72 °F occurring at 30 °F and 251 mph. For the 4×5-foot area, the minimum range is 2.67 °F with a standard deviation of 0.58 °F occurring at 30 °F and 251 mph. These minima approach the temperature variation goals. The variations tend to be much worse for temperatures above freezing. For temperatures below freezing, the variation tends to be best around 150 to 250 mph.

The temperature distribution data are extremely important in the Icing Research Tunnel, since test section total temperature variations can affect the physics of ice formation on test articles.

Effect of Air Injection Through Spray Bars

Figures 16, 17, and 18 illustrate the effects of air injection through the spray bars on test section flow quality for the years 1997 and 2000. Figures 16(a) and 16(b) show the effects on total pressure recovery, Figures 16(c) and 16(d) show the effects on static pressure recovery, and Figures 16(e) and 16(f) show the effects on total temperature recovery for $T_{D,avg}$=40 °F. These data were acquired on centerline ($Z$=36-inches), for test section velocities of 100, 200, and 300 mph, and with the spray bar air pressure set at 0 and 80 psig.

The general trend in total pressure recovery for both years is a slight increase in total pressure with air spray on. It can be seen from Figures 16(a) and 16(b) that the variation in total pressure for 1997 and 2000 is similar. The general trend in static pressure recovery is that air spray has no major effect. This is true for 5 of the 6 cases presented in Figures 16(c) and 16(d). In 1997 at 300 mph, it appears that air spray had some effect by moving he static pressure recovery curve closer to 1.0. This would be indicative of a reduction in test section air speed. It is believed that differences in the curves may be the result of smaller differences in the tunnel conditions and not solely the result of air spray. In terms of total temperature recovery, it appears that air spray had no major effect. These results can be seen in Figures 16(e) and 16(f). The variation in the recovery lines in both years is consistent with what is expected in terms of temporal variation.

Figures 17(a) through 17(d) show centerline pitch and yaw flow angle spanwise distributions for 1997 and 2000. Distributions are shown for 100, 200, and 300 mph and with and without 80 psig of air spray. Positive pitch values indicate flow toward the test section ceiling and positive yaw values indicate flow toward the outer wall. Figures 17(a) and 17(b) show the pitch results. There seems to be no significant effect with and without air spray and the variability seems to be similar for both 1997 and 2000. For the year 2000, the pitch flow angles are tending to zero for values of $Y$ greater than or equal to 24-inches. Figures 17(c) and 17(d) show the yaw results. The overall range of the 2000 yaw data is less than the 1997 yaw data. The 1997 data show no strong effect with or without air spray. For 2000, there seems to be a drop in yaw angle with air spray compared to the data without air spray for values of $Y$ greater than or equal to 60-inches. There also seems to be a change in the yaw profile shape when comparing 1997 data to 2000. This may be the result of the new heat exchanger and Corner D turning vanes. The change was not adverse; it is just interesting to note the change.

By subtracting the local test section velocity for air spray on ($V_{Pair}$ = 80 psig) from the local test section velocity for air spray off ($V_{Pair}$ = 0 psig) and plotting this difference versus the velocity for air spray off ($V_{Pair}$ = 0 psig), Figure 18 was generated. This figure includes data from 1997 and 2000. The trend is a decaying function with increasing test section air speed. The $\Delta V$ can be as large as 7 mph for low test section air speeds such as 25 mph. It would be expected that air being sprayed into the settling chamber would add momentum

and velocity to the test section. The 1997 and 2000 data do not agree very well for test section airspeeds greater than 75 mph. The differences are believed to be the result of test-to-test variability and measurement uncertainty. The reader should not be too distracted with this discrepancy.

Turbulence Intensity

Figures 19, 20, and 21 show turbulence intensity results for three spanwise locations respectively: $Y$ = 31.2, 53.7, and 76.2-inches. Within each figure, there are three sub-figures. Sub-figure (a) is axial turbulence intensity data for 1997, sub-figure (b) is axial turbulence intensity data for 2000, and sub-figure (c) is transverse turbulence intensity data for 2000. Each sub-figure has data from multiple $Z$ elevations from 9 to 69-inches. In addition, data from both single sensor (S) and dual sensor (X) hot wire probes are presented along with data for air spray in the settling chamber. The dual sensor X hot wire probes were oriented so that the probe near centerline ($Y$=53.7-inches) measured horizontal turbulence intensity and the two other probes were oriented to measure vertical turbulence intensity. In general, wind tunnel test sections have isotropic or homogeneous transverse turbulence intensity. For this reason, no distinction among the transverse turbulence intensities from the three different probes is made.

Figures 19 through 21 are intended to give the reader the complete picture of all hot wire data taken in 1997 and 2000. It is immediately apparent that the data with air spray on indicate much higher turbulence intensity than without air spray. With air spray on and with the test section air speed at 25 mph, turbulence intensities can be as high as 3 to 4%. It drops down to 0.5 to 1.5% at 250 mph with air spray on. It is also apparent at the turbulence intensities near centerline ($Y$=53.7-inches) are higher than beyond centerline ($Y$=31.2 and 76.2-inches). The reason for this may be the spray bar vertical support strut in the settling chamber. The wake from this support may persist into the test section. Beyond centerline, high turbulence intensities are seen 3-inches away from the ceiling ($Z$=69-inch). Previous boundary layer measurements in the IRT test section have shown the boundary layer on the ceiling to be about 4-inches thick.

Another general observation is that the transverse turbulence intensity data are higher than the axial intensity data. This is further shown in Table 3 where average axial ($TI_u$) and average transverse ($TI_v$) turbulence intensities are included as part of the statistical flow quality results for 100 and 200 mph and for the 4×5-foot area. At 100 mph, the average axial turbulence intensity is 0.50% and the average transverse turbulence intensity is 0.72%. For 200 mph, the average axial turbulence intensity is 0.52% and the average transverse turbulence intensity is 0.78%. With the amount of turbulence intensity data obtained, statistics could only be computed for the 4×5-foot area. Even computing summary statistics for the 4×5-foot area was a stretch. No data was available for 300 mph since the hot wire probes would not survive beyond 250 mph.

Figure 22 is a summary plot of the average axial turbulence intensities for 1997 and 2000 and the average transverse turbulence intensities for 2000. The data in this chart were averaged over 15 <= $Z$ <= 63-inches and 50 <= $V_{bellmouth}$ <= 200 mph and included only hot wire X probe data with no air spray for 2000 and only single sensor hot wire data with no air spray for 1997. From this chart is it apparent that the axial turbulence intensity was reduced by about 0.2 to 0.4% in going from the 1997 IRT configuration to the 2000 IRT configuration. It can also be seen that the average axial turbulence intensity (2000 data) meets the 0.5% turbulence intensity goal beyond centerline.

Pressure and Flow Angle Standard Deviations

Figures 23(a), (b), (c), (d), (e), and (f) present IRT test section standard deviations for total pressure, static pressure, Mach number, velocity, pitch angle, and yaw angle. The same standard deviations specified in Table 3 are plotted in Figure 23. Figure 23 gives a more complete picture of how the standard deviation of the flow parameters vary with test section air speed, with test section area (4×5 versus 6×9-foot area), and with year (1997 versus 2000).

For total pressure (Figure 23(a)), there was a general reduction in standard deviation for the 6×9-foot area from 1997 to 2000, but the results did not change for the 4×5-foot area from 1997 to 2000. For static pressure (Figure 23(b)), the standard deviation stayed the same for the 6×9-foot area from 1997 to 2000, but the standard deviation for 2000 increased for the 4×5-foot area. During the testing in 2000, a significant amount of moisture was condensing in the test section due to the continued velocity and thermal cycling of the tunnel. More moisture than was seen in 1997. This may be one possible reason for the increased static pressure variation. In reviewing the centerline static pressure profiles in Figures 16(c) and (d), it is apparent that the data show more variation in the core flow for 2000 than in 1997. It may be that the static pressure distribution may have suffered some degradation in static pressure uniformity as a result of the IRT modifications. Future measurements will either confirm or dispute these results. The static pressure recoveries in Figure 10 also show some significant variation in the core flow.

Figures 23(c) and 23(d) show the standard deviation results for Mach number and velocity. There are improvements for the 6×9-foot area in going from 1997 to 2000. This is a result of the improvements in the total pressure variation seen in Figure 23(a). For the 4×5-foot area, an increase in standard deviation is apparent in going from 1997 to 2000. This is primarily the result of the increase in the static pressure standard deviation seen in Figure 23(b). Even though there is an increase, the Mach number standard deviation flow quality goal of 0.00083 is met for test section air speeds below 300 mph and for the 4×5-foot area.

Figure 23(e) and 23(f) show the standard deviation results for pitch and yaw angle respectively. In terms of pitch angle, the standard deviation stayed about the same for the 6×9-foot area in going from 1997 to 2000. For the 4×5-foot area, there was an improvement in standard deviation. In terms of yaw angle, improvements in standard deviation are seen for both the 6×9 and 4×5-foot areas in going from 1997 to 2000. For both pitch and yaw, the flow angle standard deviation flow quality goal of 0.083 degrees was not met. It is believed that flow straightening devices such as honeycomb in the settling chamber would be necessary to approach the goal. Such devices are not possible in the IRT due to the potential problem of ice build up.

Total Temperature Standard Deviations

Figures 24(a) and 24(b) show the total temperature standard deviation results for the 6×9 and 4×5-foot areas respectively. For the year 2000, results for $T_{D,avg}$ temperatures of ambient, 40, 30, 0, and –20 °F are presented. For the year 1997, results for $T_{D,avg}$ = 40 °F are the only ones available. The standard deviations presented in Table 4 can be found on these plots. These plots show that the 1997 standard deviation at 40 °F were about 1.5 and 1.0 °F for the 6×9 and 4×5-foot areas respectively. For the 2000 data above freezing, the standard deviations were generally found to be larger than the 1997 data. For the 2000 data below freezing, the standard deviations were generally found to be less than or equal to the 1997 data. The sub-freezing 2000 data generally began to approach the 0.33 °F standard deviation temperature flow quality goal.

Calibration Curves

Figure 25 shows five calibration curves relating test section local conditions measured by the 9-foot survey rake to facility instrumentation measurements (bellmouth conditions or $T_{D,avg}$). These calibration curves will be used to provide accurate flow field conditions in the test section during research tests. Data for a centered 4×5-foot cross-section were used in constructing these calibration curves. This cross-section size was selected instead of the full 6×9-foot area to avoid wall effects and because it is more representative of the area in which research models are tested.

Figure 25(a) relates the local test section total pressure measured by the 9-foot survey rake to the total pressure measured by the two facility bellmouth rakes. Figure 25(b) relates local static pressure to bellmouth static pressure. Figure 25(c) relates local dynamic pressure to bellmouth dynamic pressure. Figure 25(d) relates local velocity to test section velocity. The more significant observation is that 1.99% of the bellmouth dynamic pressure must be added to the bellmouth dynamic pressure to predict what the local test section dynamic pressure is. Similarly, 1.48% of the bellmouth velocity must be added to the bellmouth velocity to predict what the test section velocity is.

Figure 25(e) relates local test section temperature to D corner average temperature. It can be seen from this figure that there is significant variability about the curve fit line; enough variability to say that the D corner average temperature generally predicts the local test section total temperature with a level of uncertainty quantified by the standard deviations in Figure 24 or Table 4.

Table 5 compares linear curve-fit coefficients for the 1997 calibration curves and the 2000 calibration curves. There is little change in the coefficients for total pressure and static pressure. There is a more significant change in the coefficients for temperature. In 1997, the amount of temperature data obtained was not as large as the amount of data collected for 2000. In addition, the 2000 coefficients represent temperature data from –20 °F all the way up to ambient (80°F). The 1997 coefficients represent temperature data from –20 °F to 40 °F. For this reason, some difference would be expected. In 1997, coefficients for dynamic pressure and velocity were not computed. Therefore, they are listed as "not available" (NA).

Measurement Uncertainties

Figure 26 shows the uncertainty in local total pressure, static pressure, Mach number, and velocity. Also given are uncertainties in total temperature (for the 9-foot survey rake total temperature probes and the corner D total temperature probes) and pitch and yaw flow angles. These uncertainty results along with the methodology for arriving at these uncertainties are given in Reference 7. The local total pressure uncertainty is generally about ±0.005 psi. The

uncertainty in local static pressure is generally about ±0.006 psi. Uncertainty in absolute total temperature is essentially ±2.0 °F regardless of air velocity or total temperature. For temperatures measured by thermocouples connected to the same reference block, temperature uncertainty between thermocouples is estimated to be ±0.4 °F. All thermocouples from the 9-foot survey rake were connected to the same reference block. Pitch and yaw angle uncertainties start out at ±0.5 degrees for an air velocity of 75 mph and drop down to about ±0.1 degrees at 450 mph. The local Mach number uncertainty starts out at ±0.0037 for an air velocity of 75 mph and drops down to about ±0.0007 at 450 mph. The local velocity uncertainty starts out at ±2.7 mph for an air velocity of 75 mph and drops down to about 0.6 mph at 450 mph.

## Summary and Conclusions

A test program was executed in April of 2000 to collect aerodynamic calibration and flow quality data in the NASA Glenn Icing Research Tunnel test section following the heat exchanger replacement project. This project included widening of the tunnel C-D leg, replacement of the old "W" or folded heat exchanger with a flat one, installation of new C and D corner turning vanes, and installation of fan exit guide vanes. Data were collected at a single cross-sectional plane and included total pressure, static pressure, Mach number, total temperature, flow angle, and turbulence intensity. The effects of spraying air through the water injecting spray bars on the test section flow quality were also assessed. Uncertainties for most measured parameters were documented. Calibration curves for total pressure, static pressure, dynamic pressure, velocity, and total temperature were defined.

From the results, the following conclusions were drawn:

1. For the 4×5-foot area in 2000, the maximum local total pressure standard deviation was 0.003 psi at 350 mph. The total pressure standard deviation was essentially the same in 2000 as it was in 1997 for the 4×5-foot area.
2. For the 4×5-foot area in 2000, the maximum local static pressure standard deviation was 0.011 psi at 350 mph. The static pressure standard deviation increased in 2000 over its 1997 values for the 4×5-foot area. Tunnel moisture problems may have contributed to this increase or it may just be a result of the new tunnel C-D leg.
3. For the 4×5-foot area in 2000, the maximum local Mach number and velocity standard deviations were 0.0012 and 1.05 mph respectively at 350 mph. Both standard deviations increased in 2000 over their 1997 values for the 4×5-foot area. This increase was driven by the increase in static pressure standard deviation. Even though the values increased for 2000, the Mach number standard deviations still met the 0.00083 goal for velocities less than 300 mph.
4. For the 4×5-foot area in 2000, the average pitch and yaw angle standard deviations were about 0.4 degrees. These values are improvements over the 1997 values. The 0.083 degree standard deviation flow quality goal was not met.
5. For the 4×5-foot area in 2000, the total temperature standard deviations varied between 0.5 and 1.5 °F for sub-freezing temperatures. In 2000, the standard deviation at 40 °F varied between 1.6 and 2.2 °F. In 1997, the standard deviation at 40 °F varied between 0.9 and 1.6 °F. At 40 °F, the temperature standard deviation was better in 1997 than in 2000. There wasn't enough full cross-sectional temperature data taken in 1997 (other than the 40 °F data) to make any conclusions about other temperatures. The 2000 standard deviation data for sub-freezing temperatures did approach the flow quality standard deviation goal of 0.33 °F for velocities between 150 and 250 mph.
6. Centerline temperature profiles collected over multiple temperatures (40 °F to -20 °F) did indicate much smaller spanwise temperature variability in 2000 than in 1997. The 2000 temperature data did exhibit some variability with time.
7. Average axial turbulence intensity did drop by 0.2 to 0.4% with the new tunnel modifications when compared to 1997 data. Currently, the average axial turbulence intensity is about 0.75% on vertical centerline and about 0.4% beyond vertical centerline. Transverse turbulence intensity is about 1.25% on vertical centerline and about 0.5% beyond vertical centerline. The increased intensity on centerline may be the result of the spray bar vertical support in the settling chamber. Beyond centerline, the axial and transverse turbulence intensities meet the 0.5% IRT flow quality goal.
8. Centerline measurements with and without air spray show no significant changes. There are some changes in profile shapes when comparing 1997 data to 2000, but the changes are not drastic or unexpected. In 2000, the yaw angle near the outer wall data did show a significant change with and without air spray. Test section air speed increases by 7 mph with air spray on at 80 psig and at a test section air speed of 25 mph. This increase decays to the point that the difference is below 2 mph for test section air speeds above 150 mph.

9. Satisfactory linear curve fit relationships that correlate local test section properties to bellmouth properties were presented for total pressure, static pressure, dynamic pressure, and velocity. A similar relationship was presented for the local test section total temperature, which was correlated to the D corner average temperature. The curve fit coefficients from 1997 and 2000 were compared. There were insignificant changes for total and static pressure coefficients. A significant change was seen in the total temperature coefficients. This was attributed to the fact the 2000 coefficients represent data over a much larger temperature range that the 1997 coefficients.

In general IRT flow quality goals were met for Mach number and turbulence intensity with the exceptions previously noted. Improvements were seen in pitch angle, yaw angle, and turbulence intensity with the recent IRT facility modifications. Temperature variability in 2000 approached the IRT flow quality goal for sub-freezing temperatures and medium test section air speeds.

## Recommendations

In executing the 2000 IRT aero-thermal calibration test, two items are recommended for improving the process.

1. Collect all pressure data at ambient conditions. Because moisture condensation was a problem during the 2000 tests, pressure data should only be collected at ambient conditions (60 to 90 °F). This would minimize the chances of pressure ports becoming plugged with water.
2. Fabricate a 2-dimensional total temperature probe grid for use during aero-thermal calibration. Such a grid would improve the temperature data collection efficiency. In addition, it would permit the separation of spatial and time variation in the temperature data.

If these two recommendations are implemented, overall data collection efficiency could be improved for future IRT aero-thermal calibration. All pressure data could be quickly obtained at ambient air temperatures by moving the 9-foot survey rake through its elevation range. The 2-dimensional temperature grid could then installed and all temperature data could be collected without any model changes. This would also minimize the number of velocity and temperature set points.

## References


1. Arrington, E.A., Gonsalez, J.C., and Kee-Bowling, B.A.: Flow Quality Studies of the NASA Glenn Research Center Icing Research Tunnel Circuit (1995 Tests), NASA/TM-2000-107479, March 2000.
2. Irvine, T., Kevdzija, S., Sheldon, D., and Spera, D.: Overview of the NASA Glenn Icing Research Tunnel Icing and Flow Quality Improvements Program, AIAA paper 2001-0229, January 2001.
3. Gonsalez, J.C., Arrington, E.A., and Curry, M.R.: Flow Quality Surveys of the NASA Glenn Icing Research Tunnel (2000 Tests), AIAA paper 2001-0232, January 2001.
4. Ide, R. and Oldenburg, J.: Icing Cloud Calibration of the NASA Glenn Icing Research Tunnel, AIAA paper 2001-0234, January 2001.
5. Gonsalez, J.C. and Arrington, E.A.: Aerodynamic Calibration of the NASA Lewis Icing Research Tunnel (1997 Test), AIAA paper 98-0633, January 1998.
6. Soeder, R.H., Sheldon, D.W., Andracchio, C.R., Ide, R.F., Spera, D.A., and Lalli, N.M.: NASA Lewis Icing Research Tunnel User Manual, NASA TM–107159, June 1996.
7. Gonsalez, J.C., and Arrington, E.A.: 5-Hole Flow Angle Probe Calibration for the NASA Lewis Icing Research Tunnel, AIAA Paper 96-2201, June 1996.
8. Ames Aeronautical Laboratory: Equations, Tables and Charts for Compressible Flow, NACA TR–1135 (NASA TN-1428), 1953.
9. Bruun, H.H.: Hot-Wire Anemometry, Principles and Signal Analysis, Oxford University Press, 1999.

Table 1.—Test matrix for the April 2000 test section aero-thermal calibration of the Icing Research Tunnel.

| Rake vertical position from floor, $Z$, inches | Tunnel total temperature, $T_{D,avg}$, °F | Spray bar air pressure, $P_{air}$, psig | Test section velocity, $V_{bellmouth}$, mph |
|---|---|---|---|
| 36 | 40 | 0, 80 | 0, 25, 50, 75, 100, 125, 150, 175, 200, 225, 250, 275, 300, 325, 350 |
| 36 | 70, 0, -20 | 0 | 0, 25, 50, 75, 100, 125, 150, 175, 200, 225, 250, 275, 300, 325, 350 |
| 36 | 30,20,15,10,5,-10 | 0 | 0, 50, 100, 150, 200, 250, 300, 350 |
| 6 | 70, 40 | 0 | 0, 50, 100, 150, 200, 250, 300, 350 |
| 6 | 30, 0, -20 | 0 | 0, 50, 150, 250, 350 |
| 12 | 40 | 0 | 0, 50, 100, 150, 200, 250, 300, 350 |
| 12 | 30, 0 -20 | 0 | 0, 50, 150, 250, 350 |
| 18 | 40 | 0 | 0, 50, 100, 150, 200, 250, 300, 350 |
| 18 | 30, 0 -20 | 0 | 0, 50, 150, 250, 350 |
| 24 | 70, 40 | 0 | 0, 50, 100, 150, 200, 250, 300, 350 |
| 24 | 30, 0 -20 | 0 | 0, 50, 150, 250, 350 |
| 30 | 40 | 0 | 0, 50, 100, 150, 200, 250, 300, 350 |
| 30 | 30, 0 -20 | 0 | 0, 50, 150, 250, 350 |
| 42 | 70, 40 | 0 | 0, 50, 100, 150, 200, 250, 300, 350 |
| 42 | 30, 0 -20 | 0 | 0, 50, 150, 250, 350 |
| 48 | 70, 40 | 0 | 0, 50, 100, 150, 200, 250, 300, 350 |
| 48 | 30, 0 -20 | 0 | 0, 50, 150, 250, 350 |
| 54 | 70, 40 | 0 | 0, 50, 100, 150, 200, 250, 300, 350 |
| 54 | 30, 0 -20 | 0 | 0, 50, 150, 250, 350 |
| 60 | 70, 40 | 0 | 0, 50, 100, 150, 200, 250, 300, 350 |
| 60 | 30, 0 -20 | 0 | 0, 50, 150, 250, 350 |
| 66 | 70, 40 | 0 | 0, 50, 100, 150, 200, 250, 300, 350 |
| 66 | 30, 0 -20 | 0 | 0, 50, 150, 250, 350 |

Notes:

1) The axial station was held constant at $X$=179.3-inches.
2) Test section pressure and hot wire data were only acquired at $T_{D,avg}$ temperatures of 70 and 40 °F.
3) Hot wire data were only acquired for test section velocities less than or equal to 250 mph.

Table 2.—Typical data recorded during the April 2000 aerodynamic calibration in the Icing Research Tunnel. Note, the data are for the survey rake on centerline ($Z$ = 36-inches).

| Reading | Fan speed, rpm | $P_{air}$, psig | $T_{D,avg}$, °F | $P_{T,bellmouth}$, psia | $P_{S,bellmouth}$, psia | $\Delta P_{bellmouth}$, psid | $M_{bellmouth}$ | $V_{bellmouth}$, mph |
|---|---|---|---|---|---|---|---|---|
| 655 | 0.0 | 0.1 | 60.9 | 14.430 | 14.430 | 0.000 | 0.000 | 0.0 |
| 1026 | 73.4 | 0.1 | -22.3 | 14.377 | 14.326 | 0.051 | 0.071 | 49.7 |
| 871 | 72.5 | 0.1 | -1.2 | 14.395 | 14.346 | 0.049 | 0.070 | 50.1 |
| 785 | 71.7 | 0.1 | 19.0 | 14.395 | 14.348 | 0.047 | 0.068 | 49.9 |
| 935 | 71.8 | 0.1 | 40.0 | 14.394 | 14.349 | 0.045 | 0.067 | 49.9 |
| 1997 | 72.2 | 0.1 | 63.7 | 14.313 | 14.271 | 0.043 | 0.065 | 49.9 |
| 2000 | 72.1 | 80.0 | 63.7 | 14.316 | 14.271 | 0.046 | 0.068 | 51.7 |
| 1029 | 140.1 | 0.1 | -21.1 | 14.368 | 14.163 | 0.205 | 0.143 | 100.2 |
| 877 | 138.2 | 0.1 | -2.7 | 14.389 | 14.192 | 0.197 | 0.140 | 100.1 |
| 788 | 138.2 | 0.1 | 19.7 | 14.391 | 14.203 | 0.187 | 0.137 | 100.0 |
| 943 | 139.2 | 0.1 | 40.0 | 14.389 | 14.208 | 0.181 | 0.135 | 100.4 |
| 2009 | 141.3 | 0.1 | 63.9 | 14.307 | 14.135 | 0.172 | 0.132 | 100.5 |
| 2010 | 141.3 | 80.1 | 64.1 | 14.309 | 14.129 | 0.180 | 0.135 | 102.9 |
| 1031 | 205.7 | 0.1 | -20.5 | 14.358 | 13.900 | 0.458 | 0.216 | 150.4 |
| 884 | 203.2 | 0.1 | -0.9 | 14.382 | 13.945 | 0.437 | 0.210 | 150.0 |
| 791 | 202.7 | 0.1 | 19.1 | 14.385 | 13.970 | 0.415 | 0.205 | 149.3 |
| 728 | 202.2 | 0.1 | 38.9 | 14.395 | 13.995 | 0.400 | 0.201 | 149.5 |
| 2021 | 207.7 | 0.1 | 66.2 | 14.300 | 13.920 | 0.379 | 0.196 | 150.0 |
| 2022 | 207.5 | 80.0 | 66.8 | 14.303 | 13.914 | 0.390 | 0.199 | 152.1 |
| 1036 | 269.7 | 0.0 | -20.4 | 14.347 | 13.548 | 0.799 | 0.287 | 199.7 |
| 890 | 267.4 | 0.1 | -1.4 | 14.375 | 13.606 | 0.769 | 0.281 | 199.8 |
| 792 | 268.0 | 0.1 | 20.0 | 14.378 | 13.639 | 0.739 | 0.276 | 200.3 |
| 738 | 266.6 | 0.1 | 40.2 | 14.388 | 13.679 | 0.708 | 0.270 | 200.1 |
| 2033 | 272.5 | 0.1 | 71.7 | 14.293 | 13.630 | 0.663 | 0.261 | 200.1 |
| 2034 | 272.6 | 80.7 | 72.5 | 14.296 | 13.625 | 0.671 | 0.263 | 201.5 |
| 1037 | 334.4 | 0.0 | -19.4 | 14.337 | 13.095 | 1.242 | 0.362 | 250.9 |
| 896 | 330.2 | 0.1 | -1.8 | 14.365 | 13.171 | 1.194 | 0.354 | 250.4 |
| 795 | 329.1 | 0.1 | 20.8 | 14.366 | 13.229 | 1.137 | 0.345 | 250.1 |
| 750 | 327.1 | 0.1 | 40.3 | 14.374 | 13.282 | 1.092 | 0.338 | 249.8 |
| 2045 | 336.9 | 0.0 | 79.6 | 14.282 | 13.266 | 1.015 | 0.326 | 250.7 |
| 2046 | 336.7 | 80.2 | 81.2 | 14.284 | 13.264 | 1.019 | 0.327 | 251.6 |
| 1040 | 397.7 | 0.0 | -15.4 | 14.322 | 12.576 | 1.746 | 0.435 | 300.9 |
| 902 | 394.9 | 0.1 | 0.4 | 14.349 | 12.656 | 1.693 | 0.427 | 301.0 |
| 798 | 389.9 | 0.0 | 20.0 | 14.355 | 12.752 | 1.602 | 0.415 | 298.6 |
| 989 | 391.2 | 0.0 | 40.4 | 14.350 | 12.807 | 1.544 | 0.407 | 299.1 |
| 2056 | 395.4 | 0.0 | 65.1 | 14.266 | 12.813 | 1.452 | 0.395 | 297.7 |
| 2059 | 395.4 | 80.0 | 71.3 | 14.267 | 12.839 | 1.429 | 0.391 | 296.9 |
| 1043 | 459.7 | 0.0 | -10.0 | 14.304 | 12.037 | 2.267 | 0.503 | 347.8 |
| 909 | 456.5 | 0.0 | 0.7 | 14.336 | 12.079 | 2.257 | 0.501 | 350.6 |
| 801 | 453.1 | 0.0 | 20.6 | 14.346 | 12.171 | 2.174 | 0.490 | 351.0 |
| 774 | 453.5 | 0.1 | 41.8 | 14.348 | 12.273 | 2.075 | 0.478 | 349.8 |
| 2067 | 459.9 | 0.0 | 75.6 | 14.247 | 12.324 | 1.923 | 0.460 | 348.4 |
| 2068 | 460.0 | 80.6 | 82.6 | 14.249 | 12.337 | 1.912 | 0.458 | 349.7 |

Table 3.—Aerodynamic statistical flow quality results for the Icing Research Tunnel in the year 2000.

| Area (feet) | $V_{bellmouth}$ (mph) | Parameter | Actual | | | | | Flow Quality Goals | | | |
|---|---|---|---|---|---|---|---|---|---|---|---|
| | | | Max. | Min. | Range | Average | Stnd. Dev. | Max. | Min. | Range | Stnd. Dev. |
| 6x9 | 100 | $P_{T,local}$ (psi) | 14.307 | 14.304 | 0.003 | 14.306 | 0.00053 | | | | |
| | | $P_{S,local}$ (psi) | 14.135 | 14.129 | 0.006 | 14.132 | 0.00131 | | | | |
| | | $M_{local}$ | 0.133 | 0.131 | 0.003 | 0.132 | 0.00053 | | | 0.005 | 0.00083 |
| | | Pitch (deg.) | 1.88 | -1.10 | 2.97 | 0.11 | 0.588 | 0.25 | -0.25 | 0.50 | 0.083 |
| | | Yaw (deg.) | 0.53 | -1.86 | 2.40 | -0.22 | 0.364 | 0.25 | -0.25 | 0.50 | 0.083 |
| | | $V_{local}$ (mph) | 100.96 | 99.18 | 1.78 | 100.18 | 0.39 | | | | |
| | | $TI_u$ (%) | NA | NA | NA | NA | NA | 0.50 | | | |
| | | $TI_v$ (%) | NA | NA | NA | NA | NA | 0.50 | | | |
| 4x5 | 100 | $P_{T,local}$ (psi) | 14.318 | 14.315 | 0.002 | 14.317 | 0.00052 | | | | |
| | | $P_{S,local}$ (psi) | 14.143 | 14.139 | 0.004 | 14.142 | 0.00081 | | | | |
| | | $M_{local}$ | 0.133 | 0.132 | 0.001 | 0.133 | 0.00030 | | | 0.005 | 0.00083 |
| | | Pitch (deg.) | 1.01 | -1.05 | 2.05 | -0.08 | 0.380 | 0.25 | -0.25 | 0.50 | 0.083 |
| | | Yaw (deg.) | 0.50 | -1.20 | 1.70 | -0.25 | 0.323 | 0.25 | -0.25 | 0.50 | 0.083 |
| | | $V_{local}$ (mph) | 100.95 | 99.63 | 1.33 | 100.52 | 0.22 | | | | |
| | | $TI_u$ (%) | 1.48 | 0.26 | 1.21 | 0.50 | 0.28 | 0.50 | | | |
| | | $TI_v$ (%) | 1.47 | 0.41 | 1.05 | 0.72 | 0.38 | 0.50 | | | |
| 6x9 | 200 | $P_{T,local}$ (psi) | 14.311 | 14.281 | 0.030 | 14.295 | 0.00303 | | | | |
| | | $P_{S,local}$ (psi) | 13.621 | 13.596 | 0.024 | 13.607 | 0.00492 | | | | |
| | | $M_{local}$ | 0.268 | 0.263 | 0.005 | 0.266 | 0.00095 | | | 0.005 | 0.00083 |
| | | Pitch (deg.) | 2.75 | -1.19 | 3.94 | 0.21 | 0.653 | 0.25 | -0.25 | 0.50 | 0.083 |
| | | Yaw (deg.) | 1.12 | -1.40 | 2.51 | -0.20 | 0.404 | 0.25 | -0.25 | 0.50 | 0.083 |
| | | $V_{local}$ (mph) | 202.98 | 199.52 | 3.45 | 201.50 | 0.68 | | | | |
| | | $TI_u$ (%) | NA | NA | NA | NA | NA | 0.50 | | | |
| | | $TI_v$ (%) | NA | NA | NA | NA | NA | 0.50 | | | |
| 4x5 | 200 | $P_{T,local}$ (psi) | 14.313 | 14.292 | 0.021 | 14.306 | 0.00191 | | | | |
| | | $P_{S,local}$ (psi) | 13.621 | 13.607 | 0.014 | 13.615 | 0.00299 | | | | |
| | | $M_{local}$ | 0.268 | 0.265 | 0.004 | 0.267 | 0.00062 | | | 0.005 | 0.00083 |
| | | Pitch (deg.) | 1.32 | -0.79 | 2.11 | 0.00 | 0.409 | 0.25 | -0.25 | 0.50 | 0.083 |
| | | Yaw (deg.) | 1.12 | -1.40 | 2.51 | -0.23 | 0.412 | 0.25 | -0.25 | 0.50 | 0.083 |
| | | $V_{local}$ (mph) | 202.94 | 199.77 | 3.17 | 201.82 | 0.43 | | | | |
| | | $TI_u$ (%) | 1.01 | 0.31 | 0.70 | 0.52 | 0.22 | 0.50 | | | |
| | | $TI_v$ (%) | 1.62 | 0.46 | 1.17 | 0.78 | 0.43 | 0.50 | | | |
| 6x9 | 300 | $P_{T,local}$ (psi) | 14.283 | 14.253 | 0.030 | 14.271 | 0.00312 | | | | |
| | | $P_{S,local}$ (psi) | 12.785 | 12.737 | 0.048 | 12.762 | 0.01026 | | | | |
| | | $M_{local}$ | 0.406 | 0.399 | 0.006 | 0.403 | 0.00139 | | | 0.005 | 0.00083 |
| | | Pitch (deg.) | 2.04 | -1.12 | 3.16 | 0.18 | 0.648 | 0.25 | -0.25 | 0.50 | 0.083 |
| | | Yaw (deg.) | 0.64 | -1.31 | 1.96 | -0.25 | 0.336 | 0.25 | -0.25 | 0.50 | 0.083 |
| | | $V_{local}$ (mph) | 305.57 | 300.25 | 5.31 | 303.51 | 1.19 | | | | |
| | | $TI_u$ (%) | NA | NA | NA | NA | NA | 0.50 | | | |
| | | $TI_v$ (%) | NA | NA | NA | NA | NA | 0.50 | | | |
| 4x5 | 300 | $P_{T,local}$ (psi) | 14.294 | 14.269 | 0.025 | 14.283 | 0.00295 | | | | |
| | | $P_{S,local}$ (psi) | 12.778 | 12.742 | 0.036 | 12.762 | 0.00669 | | | | |
| | | $M_{local}$ | 0.407 | 0.402 | 0.005 | 0.404 | 0.00090 | | | 0.005 | 0.00083 |
| | | Pitch (deg.) | 1.11 | -0.96 | 2.07 | -0.05 | 0.424 | 0.25 | -0.25 | 0.50 | 0.083 |
| | | Yaw (deg.) | 0.51 | -1.31 | 1.82 | -0.29 | 0.327 | 0.25 | -0.25 | 0.50 | 0.083 |
| | | $V_{local}$ (mph) | 305.64 | 302.35 | 3.28 | 304.27 | 0.81 | | | | |
| | | $TI_u$ (%) | NA | NA | NA | NA | NA | 0.50 | | | |
| | | $TI_v$ (%) | NA | NA | NA | NA | NA | 0.50 | | | |

Table 4.—Total temperature statistical results for the IRT test section in the year 2000.

| Area (feet) | $V_{bellmouth}$ (mph) | $T_{D,avg}$ (°F) | $T_{local}$ (°F) - Actual | | | | | $T_{local}$ (°F) - Goals | |
|---|---|---|---|---|---|---|---|---|---|
| | | | Max. | Min. | Range | Average | Stnd. Dev. | Range | Stnd. Dev. |
| 6x9 | 50 | 55.56 | 62.31 | 53.17 | 9.15 | 56.74 | 2.07 | 2.00 | 0.33 |
| | 150 | 57.12 | 59.03 | 52.30 | 6.73 | 57.64 | 1.10 | | |
| | 250 | 62.18 | 67.52 | 56.56 | 10.95 | 63.90 | 1.83 | | |
| | 350 | 70.53 | 80.54 | 66.67 | 13.87 | 74.47 | 3.47 | | |
| | 50 | 39.83 | 44.75 | 31.28 | 13.47 | 40.52 | 2.15 | | |
| | 150 | 39.80 | 44.13 | 32.42 | 11.70 | 39.89 | 2.00 | | |
| | 250 | 41.01 | 47.95 | 30.38 | 17.57 | 41.03 | 2.79 | | |
| | 350 | 43.67 | 47.58 | 36.98 | 10.60 | 42.70 | 2.25 | | |
| | 50 | 28.32 | 29.34 | 22.67 | 6.67 | 27.50 | 1.11 | | |
| | 150 | 29.05 | 33.24 | 26.55 | 6.69 | 28.94 | 0.86 | | |
| | 251 | 30.41 | 33.10 | 28.24 | 4.86 | 30.28 | 0.72 | | |
| | 349 | 31.31 | 34.71 | 28.03 | 6.68 | 30.53 | 1.22 | | |
| | 50 | -1.29 | 4.79 | -5.92 | 10.71 | -2.20 | 1.63 | | |
| | 150 | -0.69 | 2.75 | -3.51 | 6.26 | -1.05 | 1.08 | | |
| | 250 | 0.54 | 3.55 | -2.00 | 5.55 | 0.10 | 1.05 | | |
| | 349 | 1.15 | 4.52 | -1.35 | 5.87 | 1.09 | 1.23 | | |
| | 50 | -22.97 | -15.45 | -28.61 | 13.17 | -24.58 | 1.79 | | |
| | 150 | -22.14 | -16.40 | -24.92 | 8.52 | -22.40 | 1.39 | | |
| | 251 | -18.89 | -13.06 | -20.19 | 7.13 | -18.40 | 1.06 | | |
| | 348 | -10.43 | -6.59 | -12.51 | 5.92 | -9.54 | 1.02 | | |
| 4x5 | 50 | 55.17 | 61.92 | 53.90 | 8.02 | 56.56 | 1.94 | 2.00 | 0.33 |
| | 150 | 57.03 | 58.93 | 52.71 | 6.21 | 57.71 | 1.01 | | |
| | 250 | 61.93 | 67.26 | 58.46 | 8.80 | 64.00 | 1.72 | | |
| | 350 | 69.14 | 79.13 | 65.56 | 13.57 | 73.59 | 3.65 | | |
| | 50 | 39.27 | 44.13 | 30.73 | 13.39 | 39.98 | 2.21 | | |
| | 150 | 39.51 | 43.41 | 32.14 | 11.27 | 39.81 | 1.61 | | |
| | 250 | 40.63 | 47.57 | 34.78 | 12.78 | 41.34 | 2.00 | | |
| | 350 | 43.78 | 47.69 | 37.62 | 10.07 | 43.71 | 1.80 | | |
| | 50 | 28.22 | 29.24 | 25.12 | 4.12 | 27.71 | 0.79 | | |
| | 150 | 29.18 | 31.35 | 27.78 | 3.57 | 28.98 | 0.53 | | |
| | 251 | 30.63 | 31.74 | 29.07 | 2.67 | 30.43 | 0.58 | | |
| | 349 | 31.14 | 34.54 | 28.16 | 6.38 | 30.27 | 1.16 | | |
| | 50 | -1.43 | 0.07 | -5.49 | 5.57 | -2.53 | 1.38 | | |
| | 150 | -0.89 | 2.45 | -3.71 | 6.15 | -1.40 | 0.94 | | |
| | 250 | 0.39 | 2.33 | -2.08 | 4.41 | -0.10 | 0.88 | | |
| | 349 | 1.06 | 4.43 | -0.70 | 5.13 | 1.23 | 1.29 | | |
| | 50 | -22.92 | -20.82 | -28.43 | 7.61 | -24.57 | 1.61 | | |
| | 150 | -22.22 | -19.00 | -24.28 | 5.28 | -22.77 | 0.84 | | |
| | 251 | -18.92 | -15.08 | -19.84 | 4.76 | -18.56 | 0.71 | | |
| | 348 | -10.21 | -6.37 | -11.51 | 5.14 | -8.99 | 0.92 | | |

Table 5.—IRT test section calibration curve coefficients.
Equation is: (local parameter) = intercept + slope*(bellmouth parameter)

| Parameter | Intercept | | Slope | |
|---|---|---|---|---|
| | 1997 | 2000 | 1997 | 2000 |
| Total pressure, $P_T$ | 0.04610 psia | 0.03905 psia | 0.9969 psia/psia | 0.9973 psia/psia |
| Static pressure, $P_S$ | -0.3216 psia | -0.2761 psia | 1.0226 psia/psia | 1.0193 psia/psia |
| Dynamic pressure, $q$ | NA | -0.001675 psi | NA | 1.0199 psi/psi |
| Velocity, $V$ | NA | -1.3506 ft/sec | NA | 1.0148 (ft/sec)/(ft/sec) |
| Total temperature, $T_T$ | 0.6019 °F | -0.5115 °F | 0.9694 (°F / °F) | 1.0314 (°F / °F) |

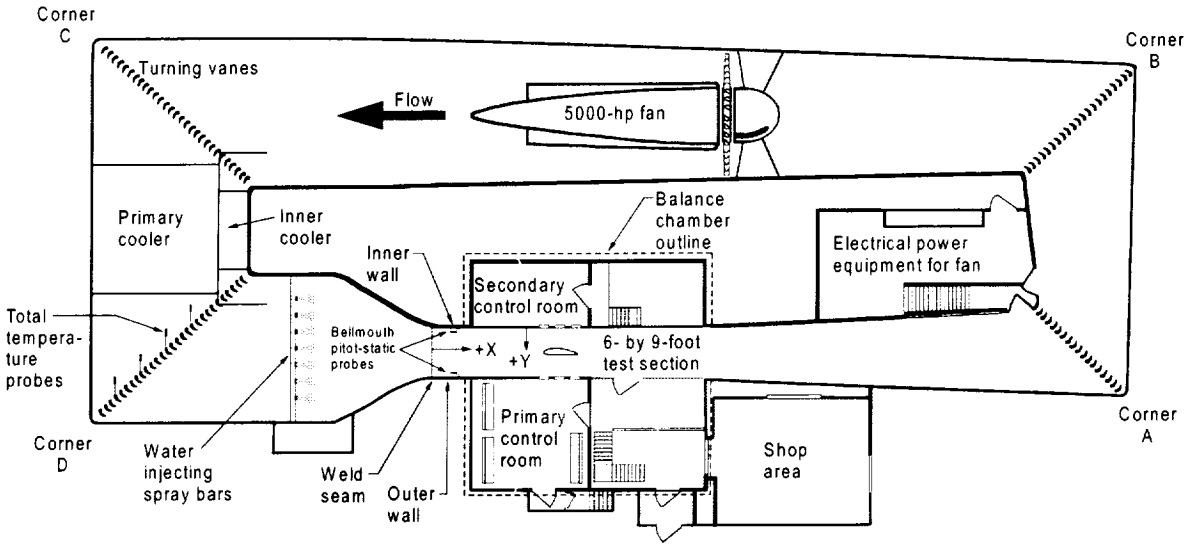


Figure 1.—April 1997 planview of the "old" NASA Glenn Icing Research Tunnel.

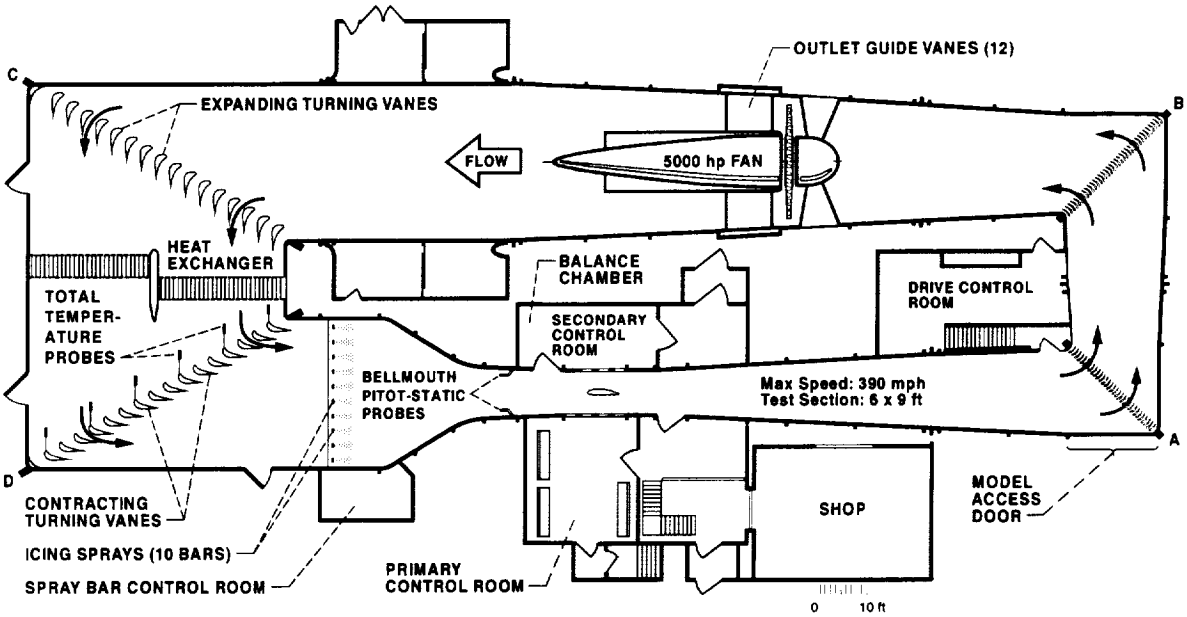


Figure 2.—April 2000 planview of the "modified" NASA Glenn Icing Research Tunnel.

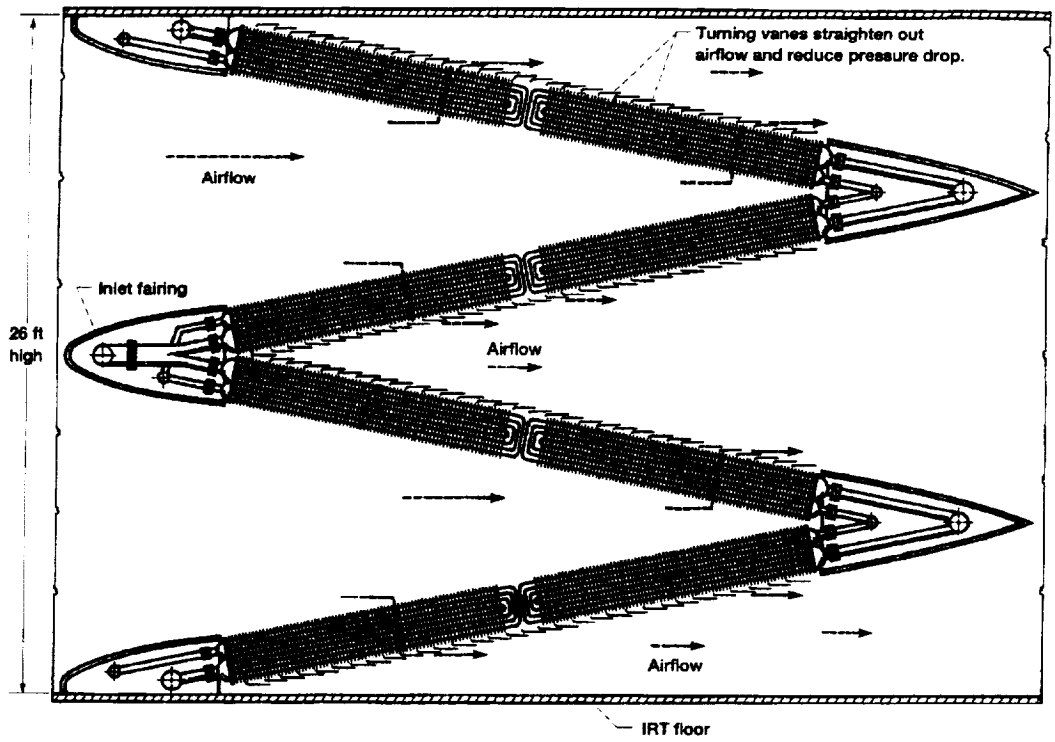


Figure 3.—April 1997 elevation view of the old IRT "W" (primary) cooler or heat exchanger.

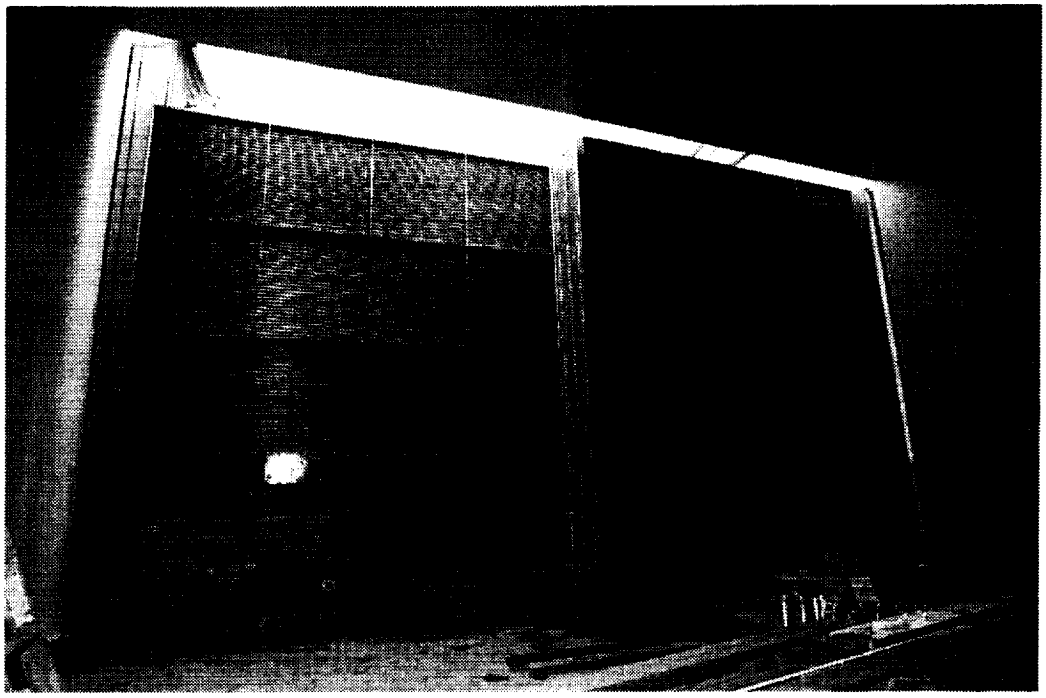

Figure 4.—April 2000 elevation view of the new IRT "flat" cooler or heat exchanger.

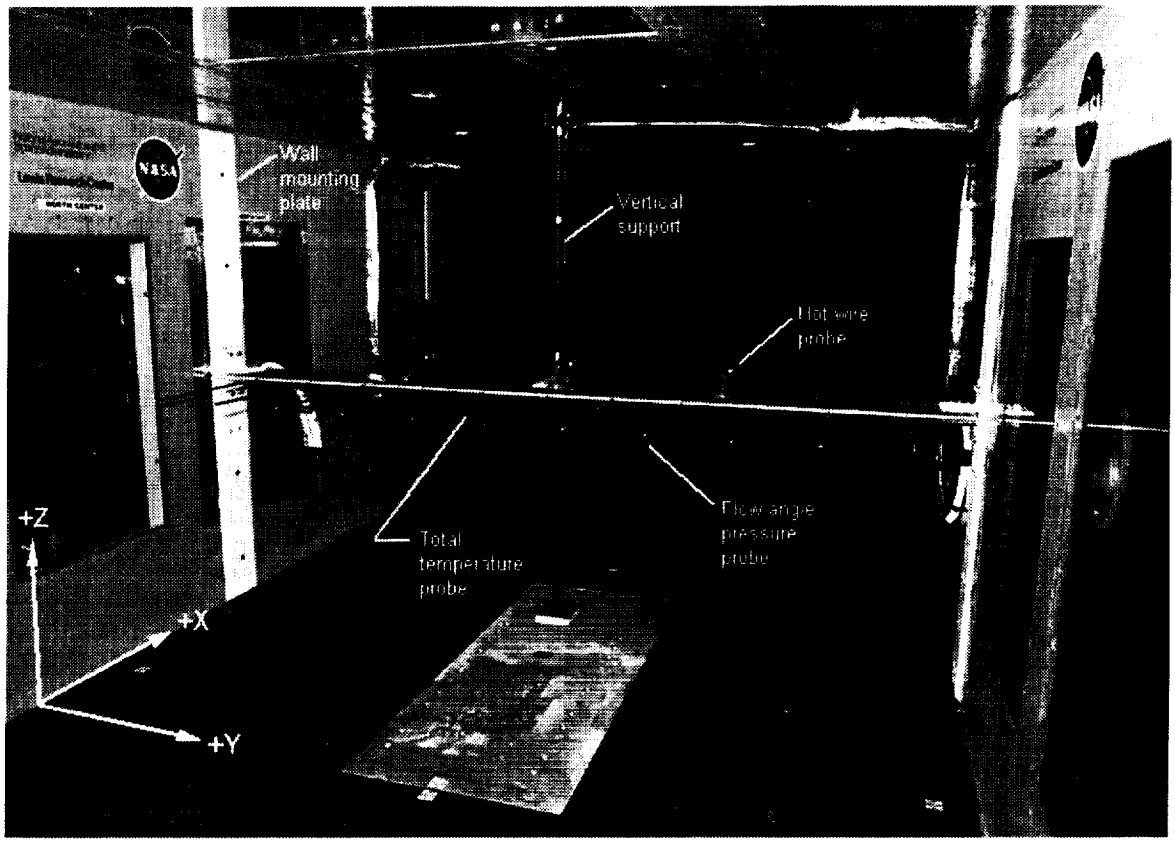


Figure 5.—Photograph of the 9-foot horizontal survey rake installed in the IRT test section for both the April 1997 and April 2000 tests.

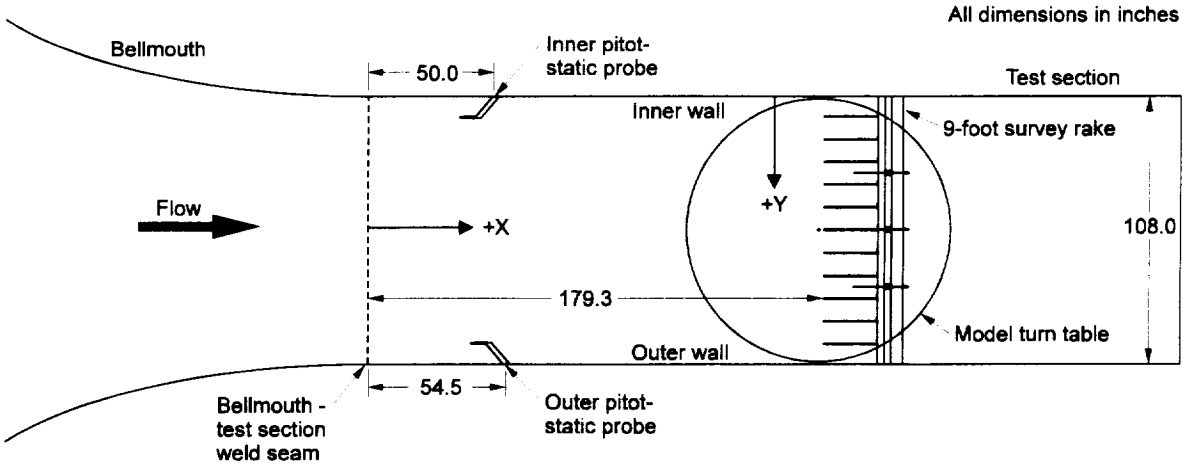


Figure 6.—Exploded planview of the IRT test section showing the 9-foot horizontal rake installed for both the April 1997 and April 2000 tests.

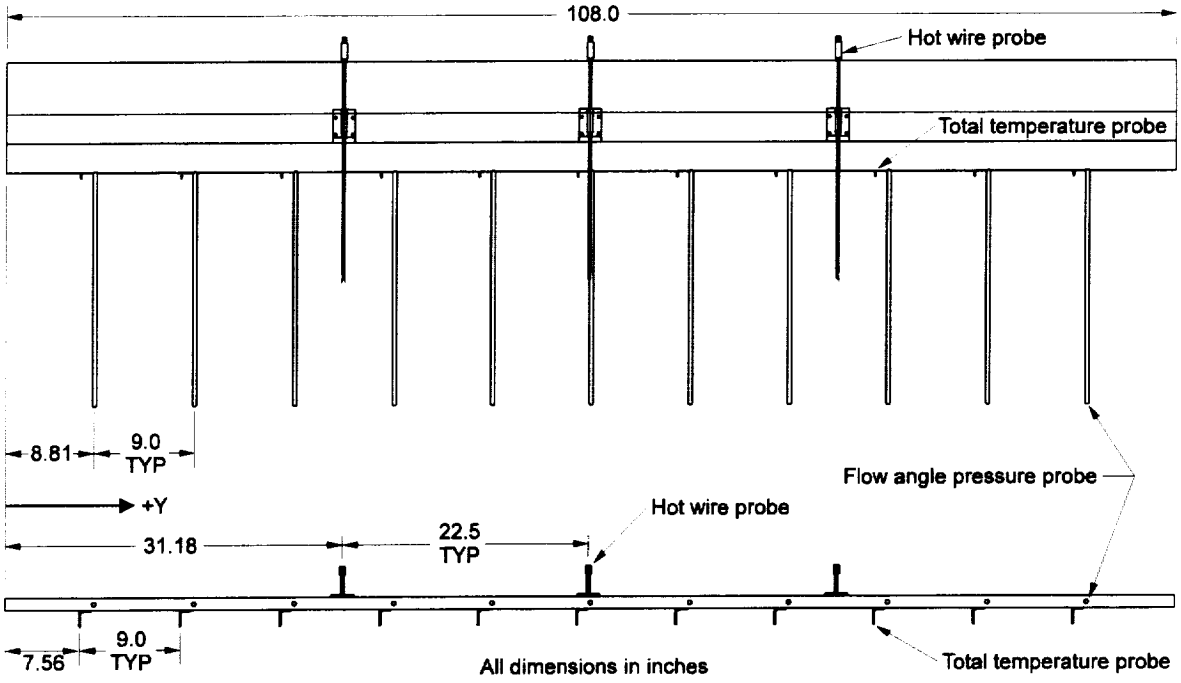


Figure 7.—Plan and front views of the 9-foot horizontal survey rake.

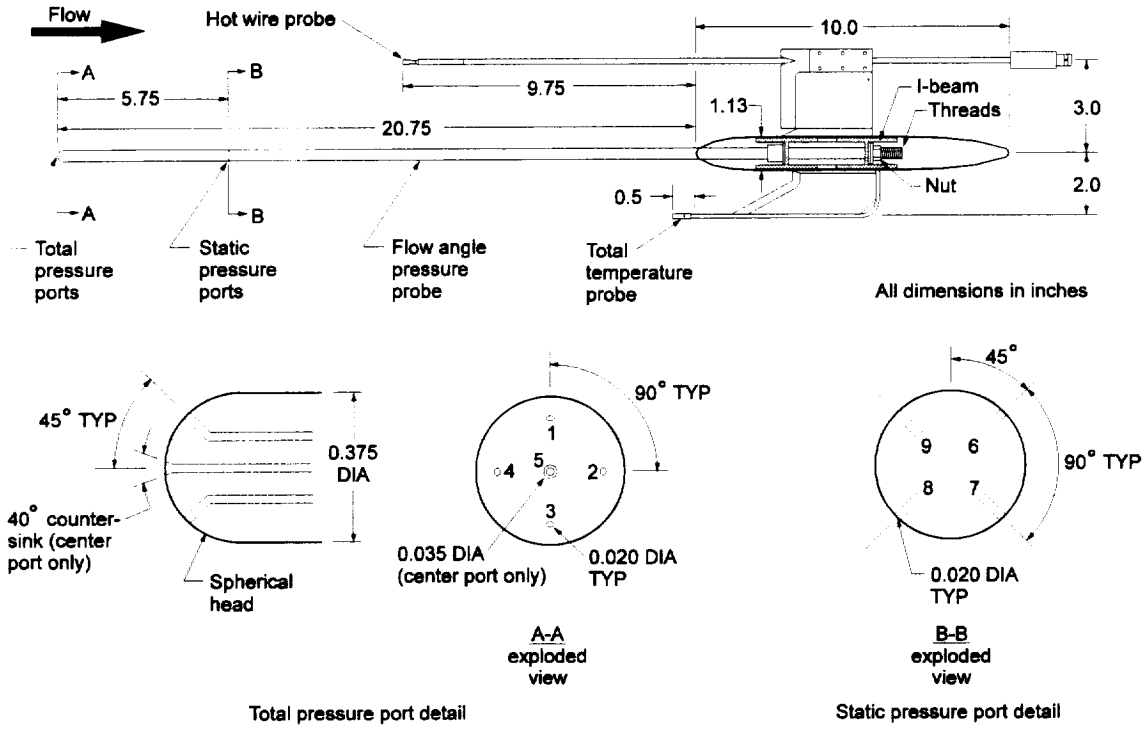


Figure 8.—Cross section view of the 9-foot horizontal rake with exploded views of the flow angle pressure probe ports.

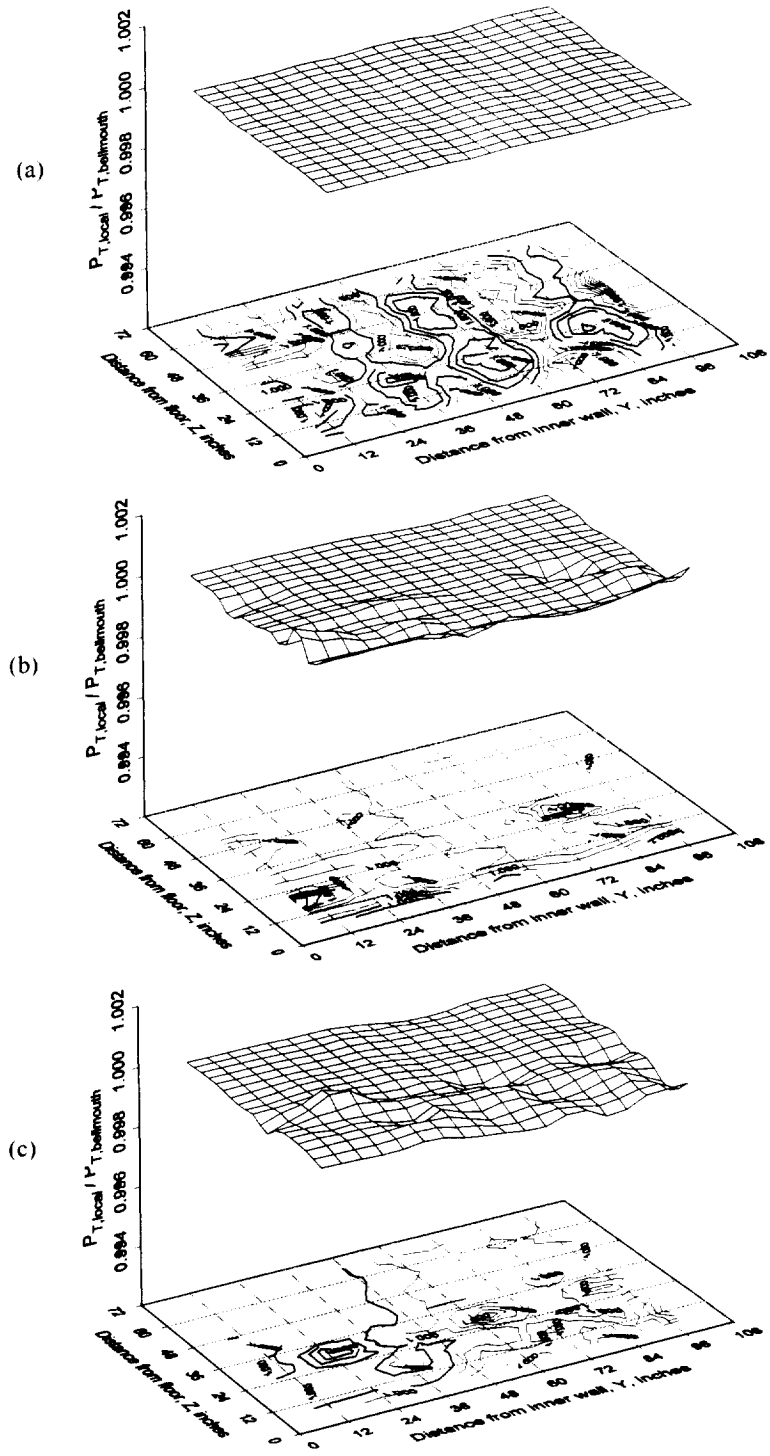


Figure 9.—April 2000 test section total pressure recovery for test section velocities of (a) 100 mph, (b) 200 mph, and (c) 300 mph.

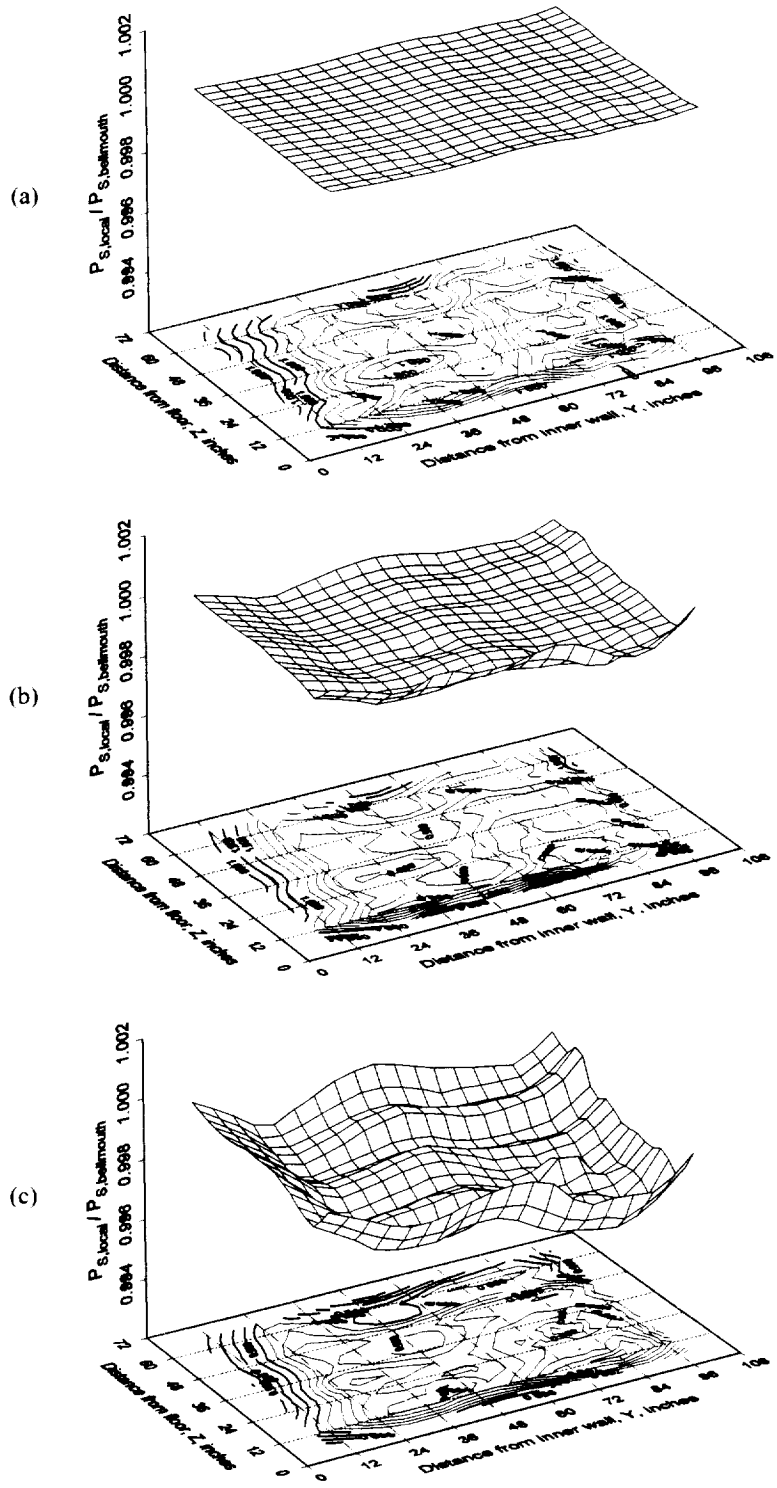


Figure 10.—April 2000 test section static pressure recovery for test section velocities of (a) 100 mph, (b) 200 mph, and (c) 300 mph.

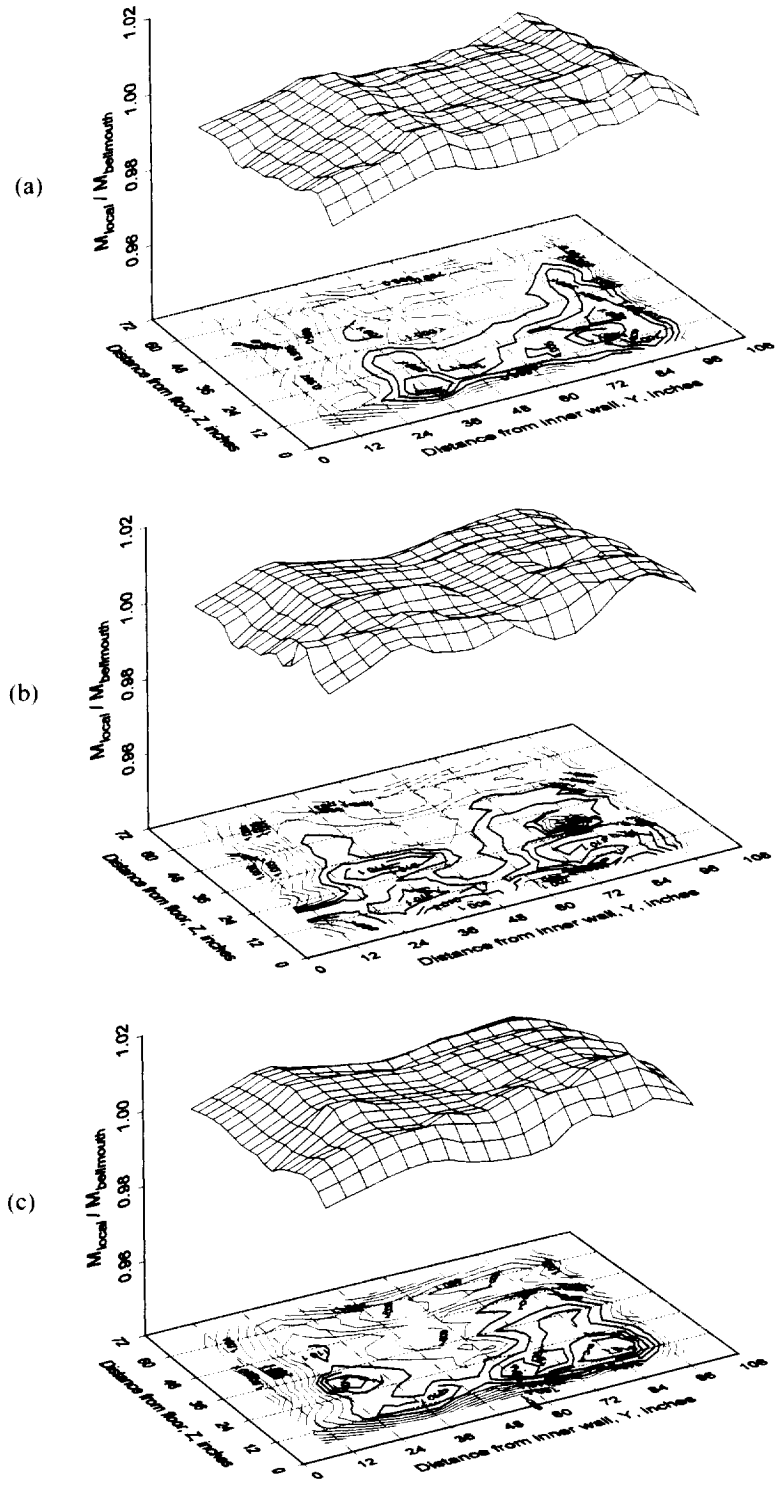


Figure 11.—April 2000 test section Mach number recovery for test section velocities of (a) 100 mph, (b) 200 mph, and (c) 300 mph.

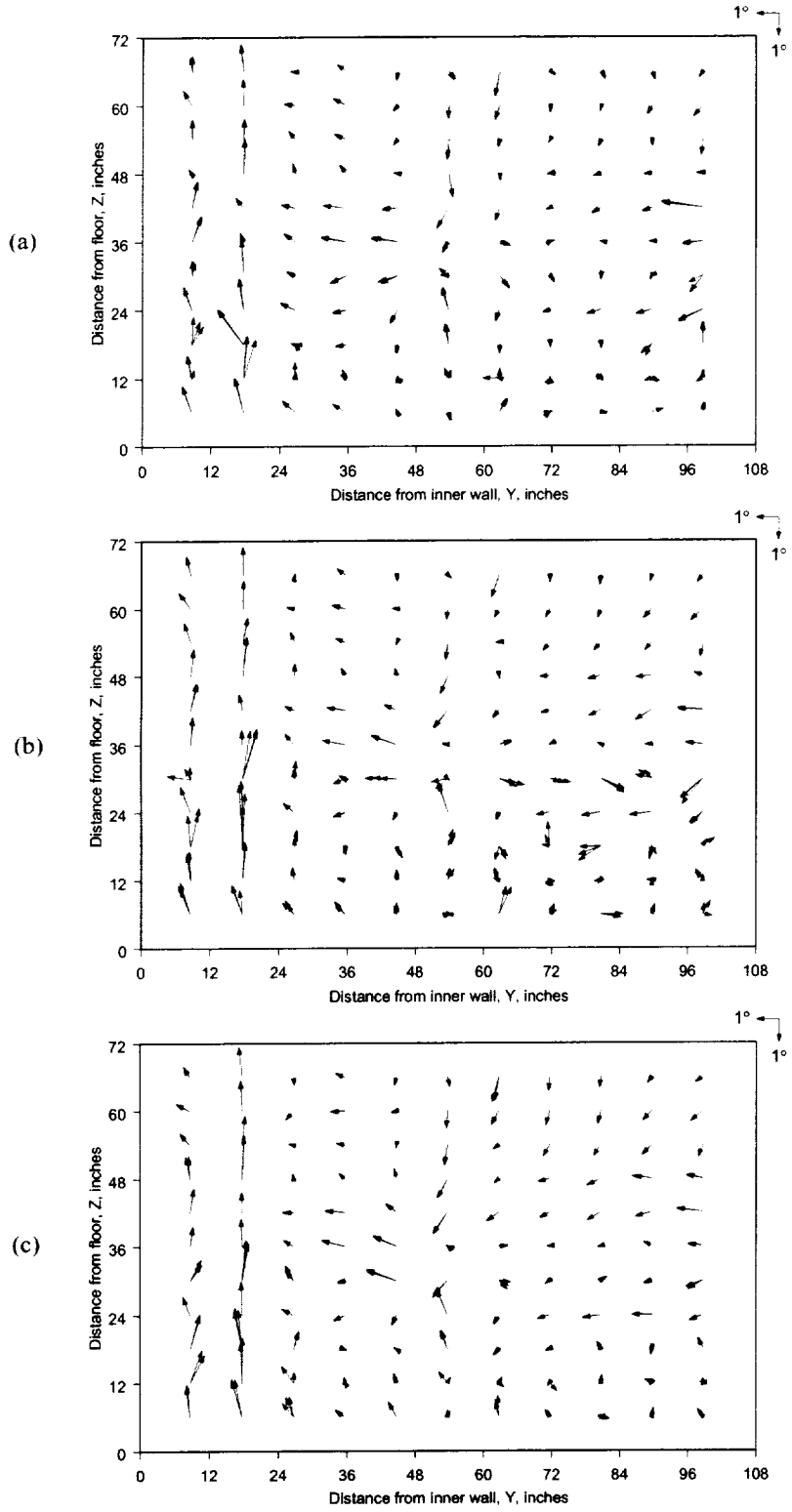


Figure 12.—April 2000 test section flow angle vectors for test section velocities of (a) 100 mph, (b) 200 mph, and (c) 300 mph.

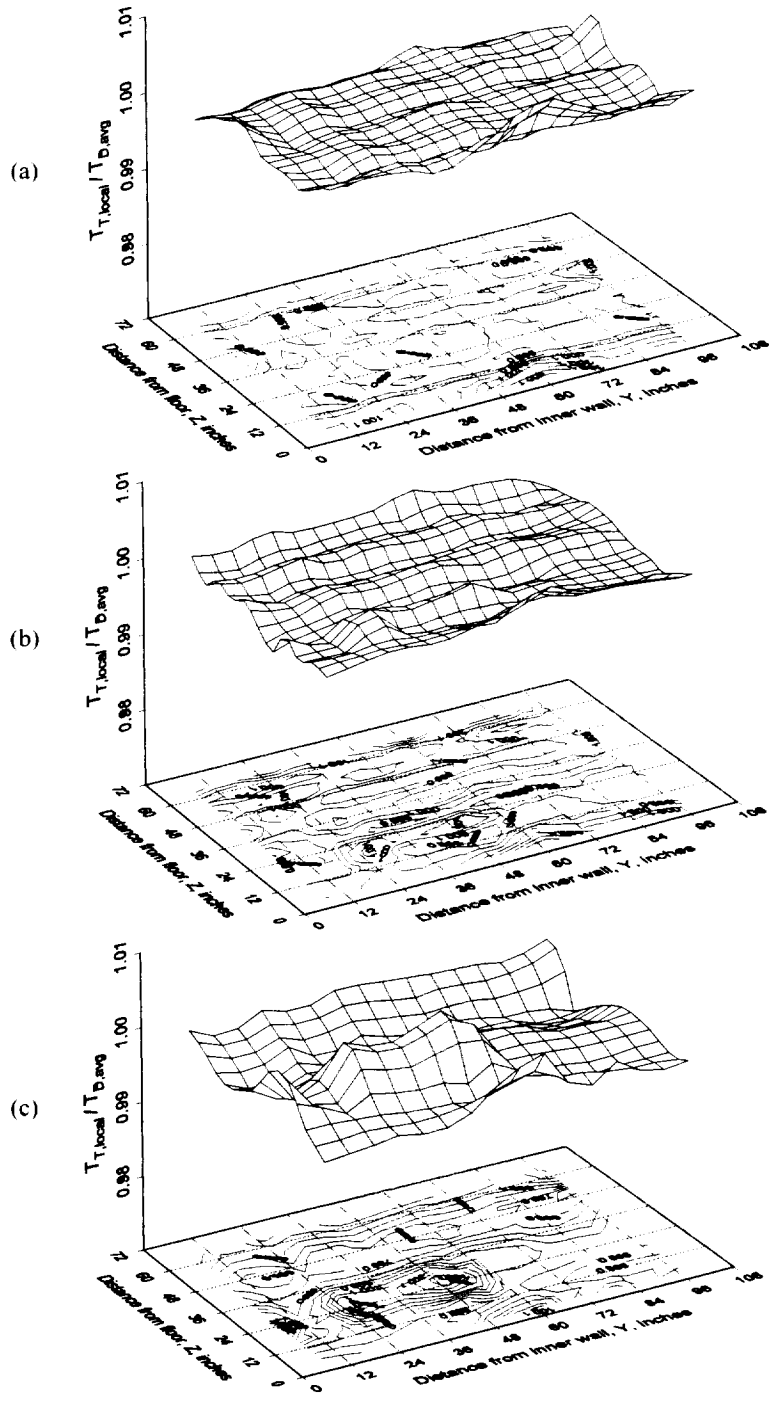


Figure 13.—April 2000 test section total temperature recovery for $T_{D,avg}$ = 30 °F and for test section velocities of (a) 150 mph, (b) 250 mph, and (c) 350 mph.

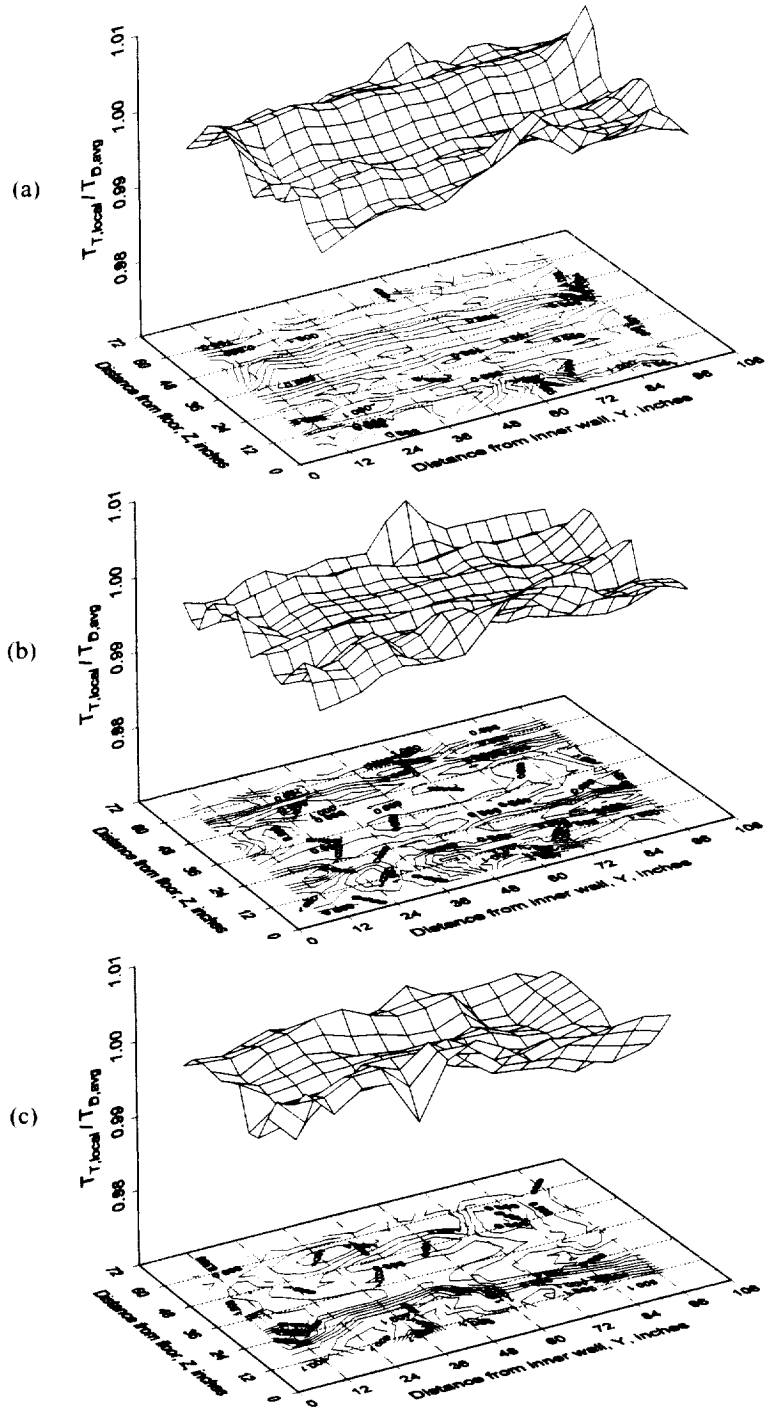


Figure 14.—April 2000 test section total temperature recovery for $T_{D,avg}$ = 0 °F and for test section velocities of (a) 150 mph, (b) 250 mph, and (c) 350 mph.

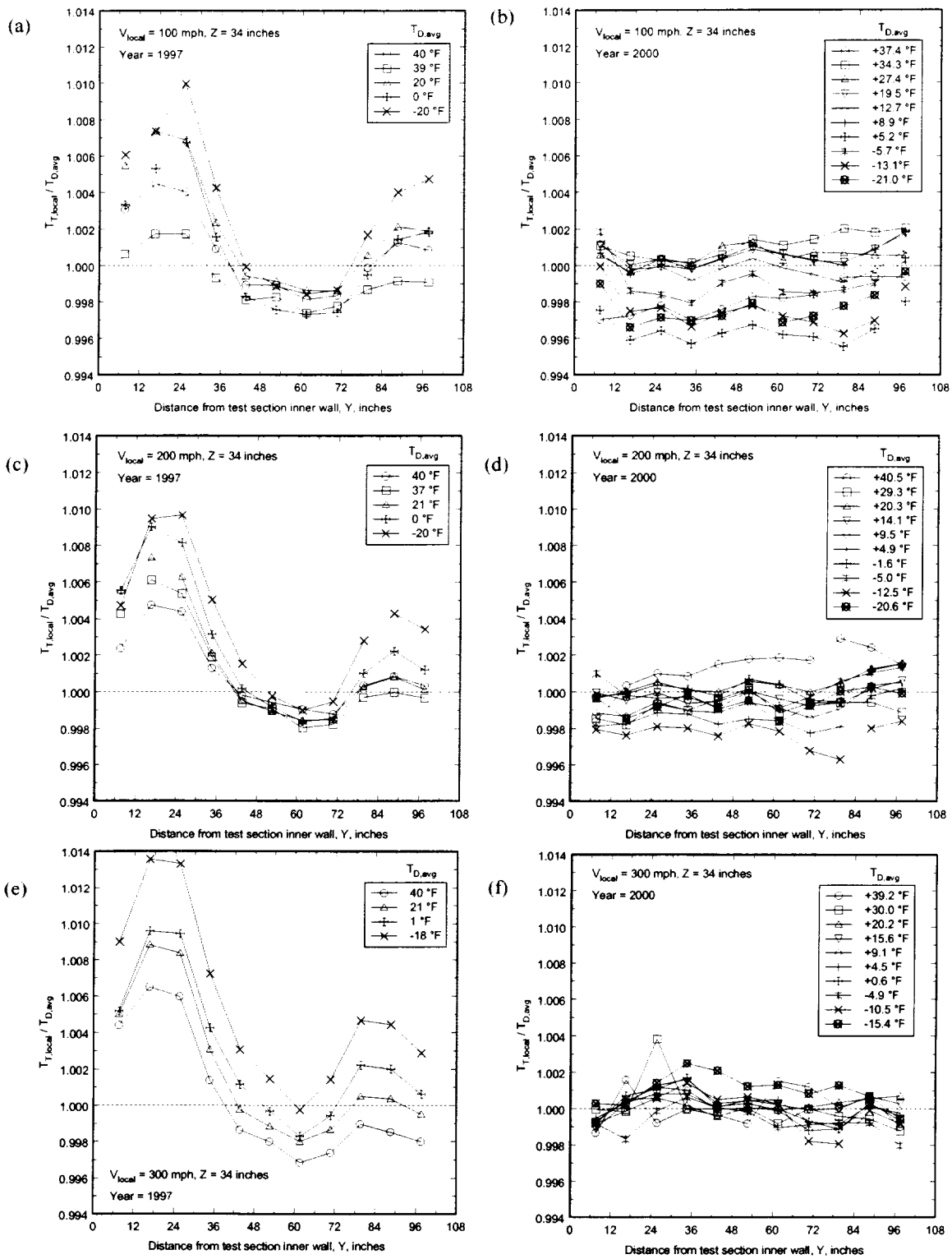


Figure 15.—Centerline total temperature recovery profiles for multiple $T_{D,avg}$ temperatures and for years and test section velocities as follows: (a) 1997, 100 mph, (b) 2000, 100 mph, (c) 1997, 200 mph, (d) 2000, 200 mph, (e) 1997, 300 mph, (f) 2000, 300 mph.

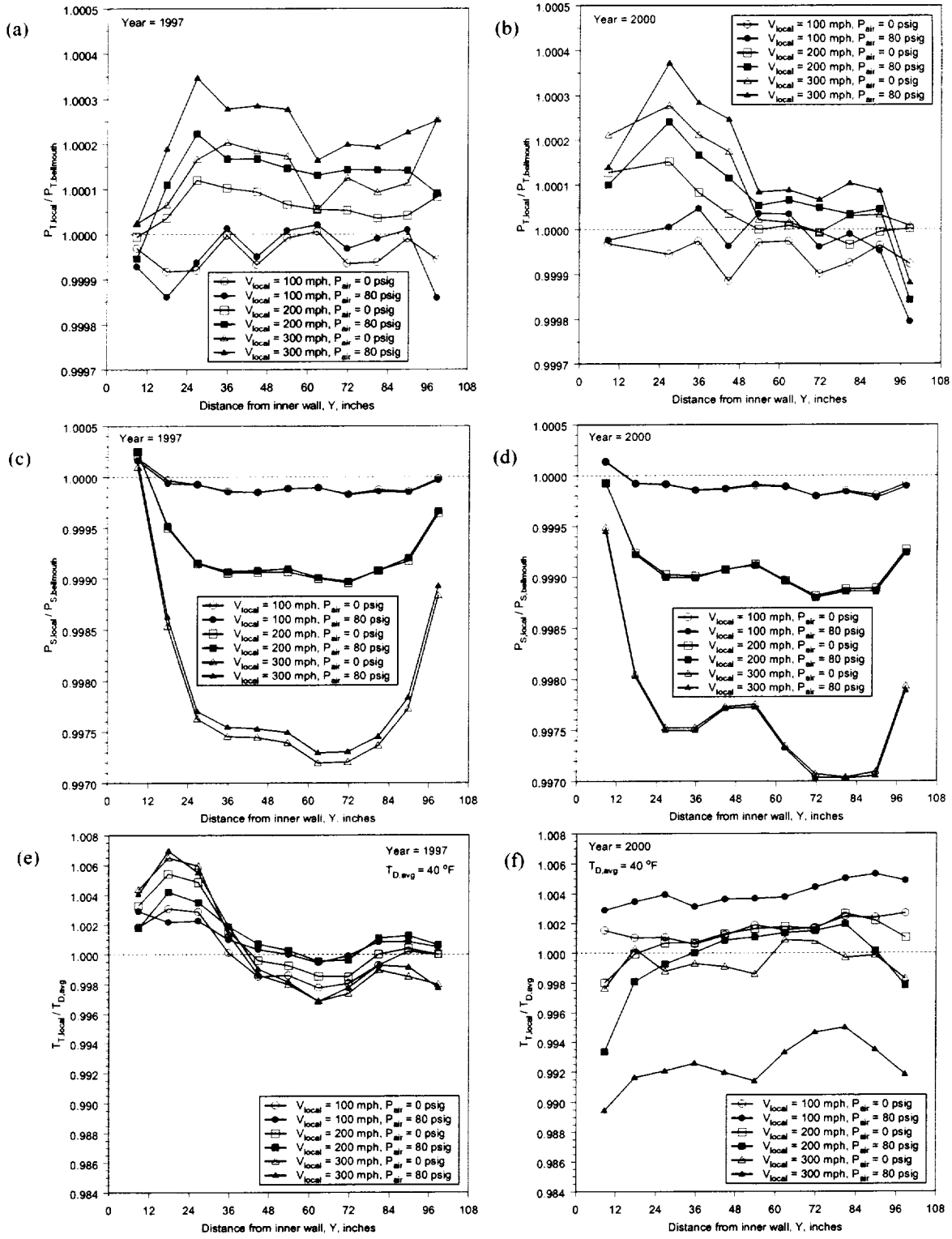


Figure 16.—Comparison of centerline horizontal profiles with and without 80 psig air spray for the years and parameters as follows: (a) 1997, total pressure, (b) 2000, total pressure, (c) 1997, static pressure, (d) 2000, static pressure, (e) 1997, total temperature, (f) 2000, total temperature.

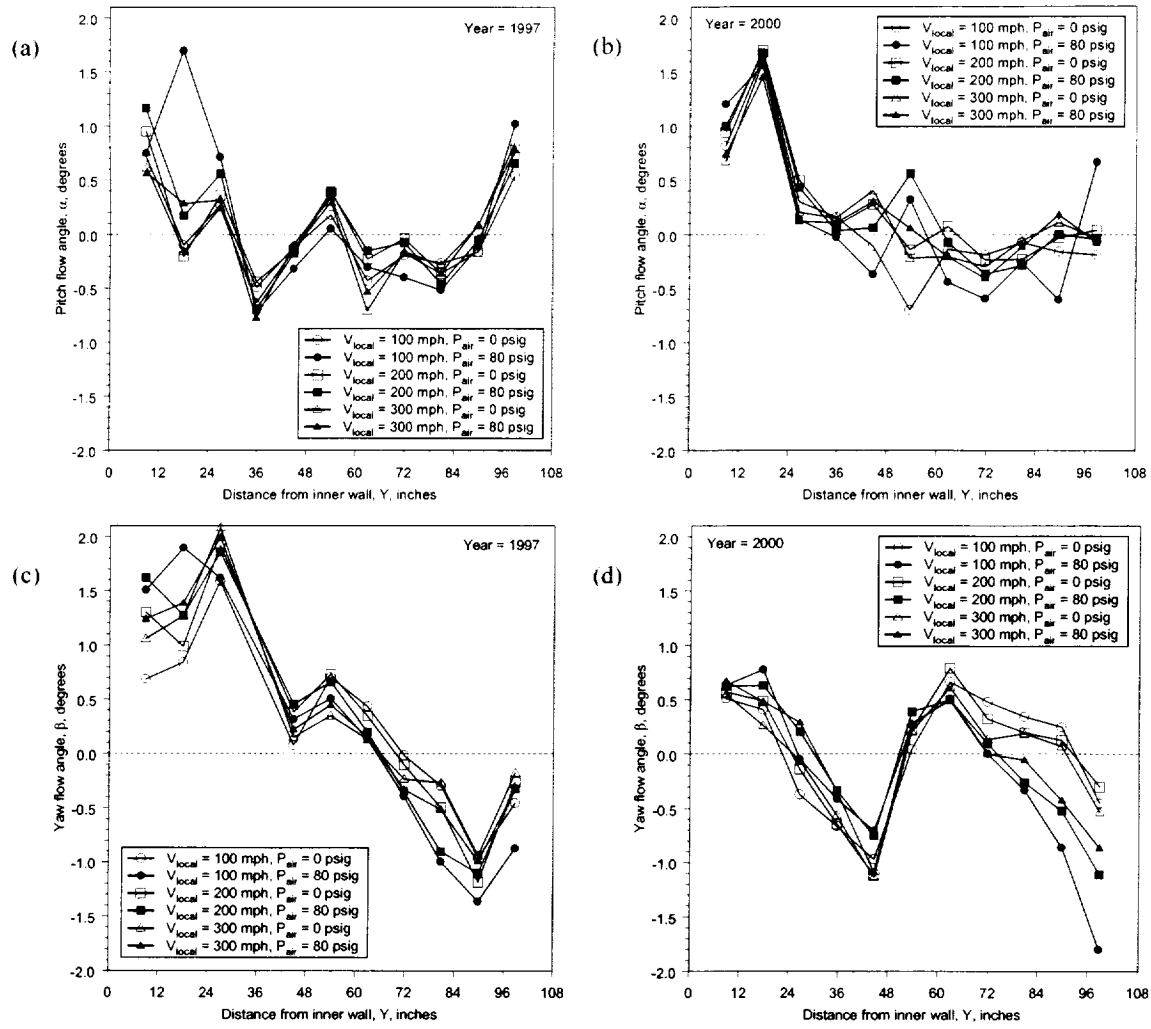


Figure 17.—Comparison of centerline horizontal profiles with and without 80 psig air spray for the years and parameters as follows: (a) 1997, pitch flow angle, (b) 2000, pitch flow angle, (c) 1997, yaw flow angle, (d) 2000, yaw flow angle.

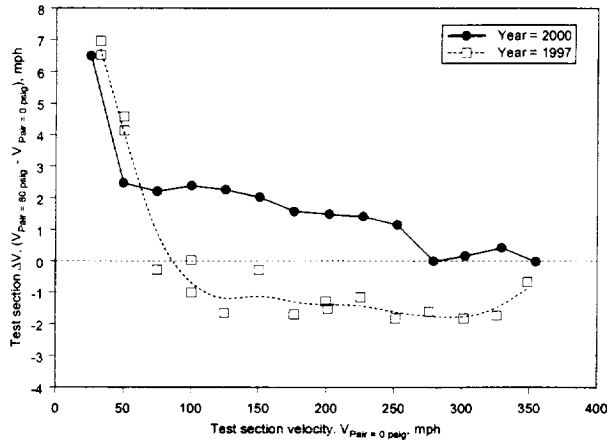


Figure 18.—Change in test section velocity as a result of 80 psig air spray.

(a)

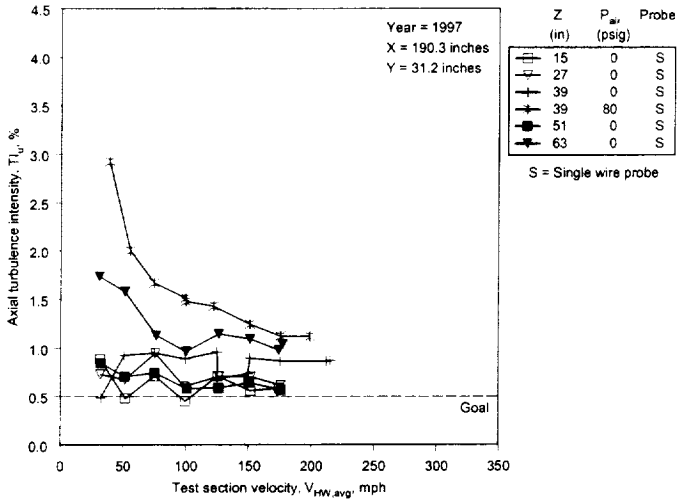


(b)

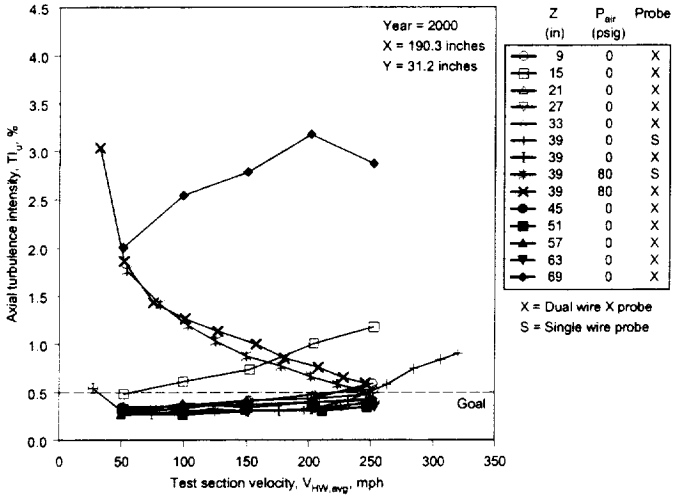


(c)

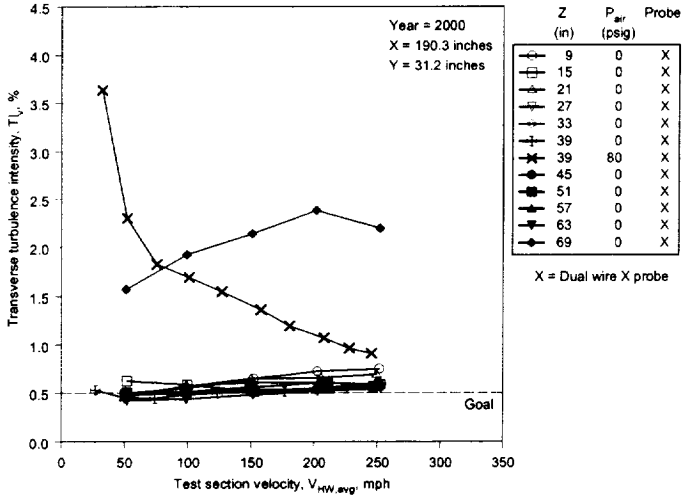


Figure 19.—Hot wire turbulence intensity data for $Y$=31.2 inches and for the years and parameters as follows: (a) 1997, axial turbulence intensity, (b) 2000, axial turbulence intensity, and (c) 2000, transverse (horizontal) turbulence intensity.

(a)

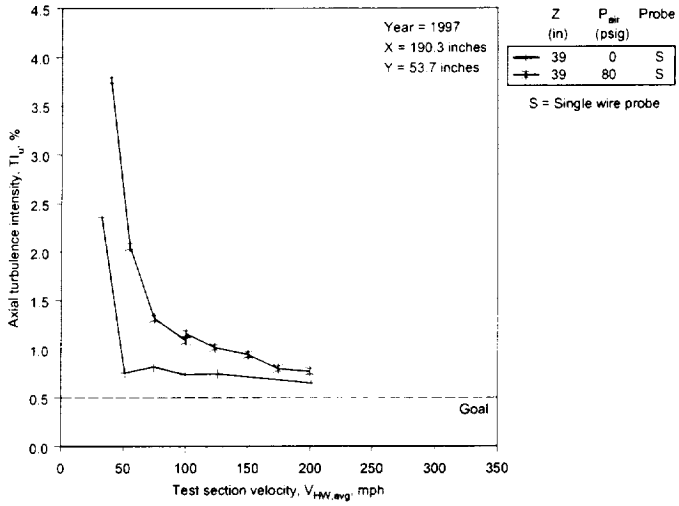


(b)

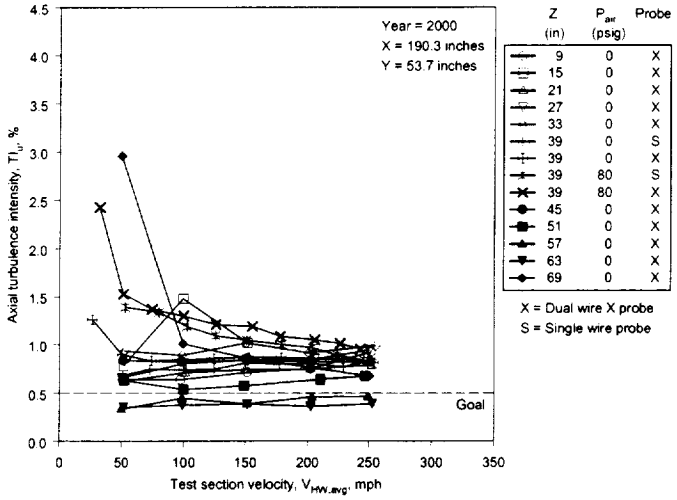


(c)

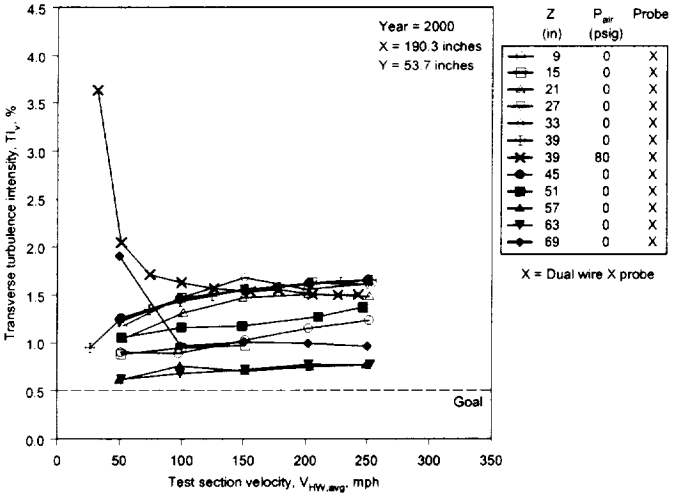


Figure 20.—Hot wire turbulence intensity data for $Y$=53.7 inches and for the years and parameters as follows: (a) 1997, axial turbulence intensity, (b) 2000, axial turbulence intensity, and (c) 2000, transverse turbulence intensity.

(a)

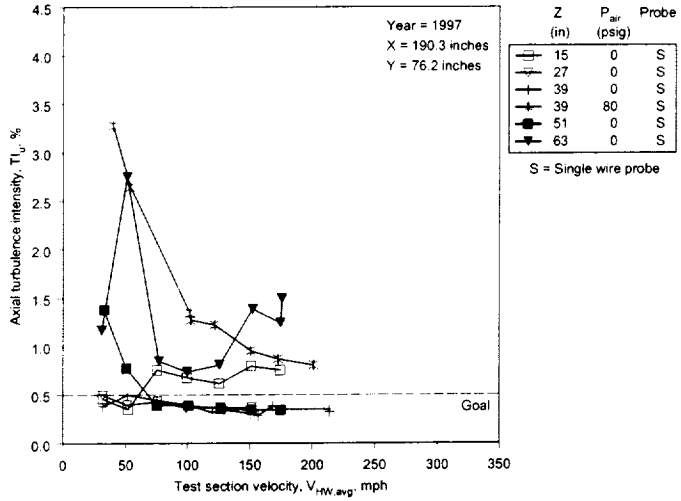


(b)

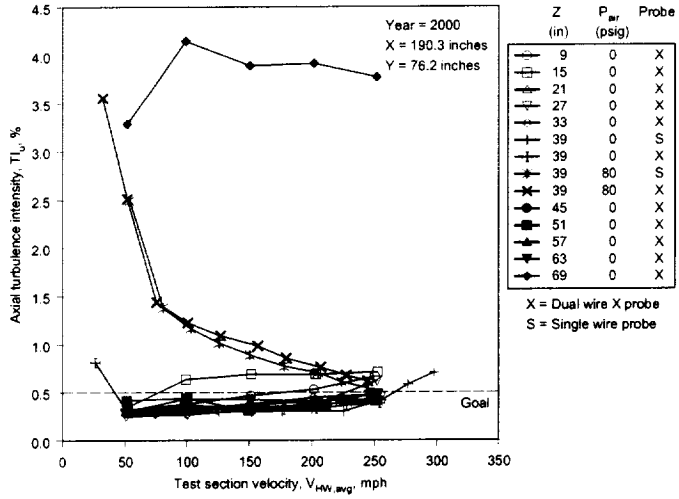


(c)

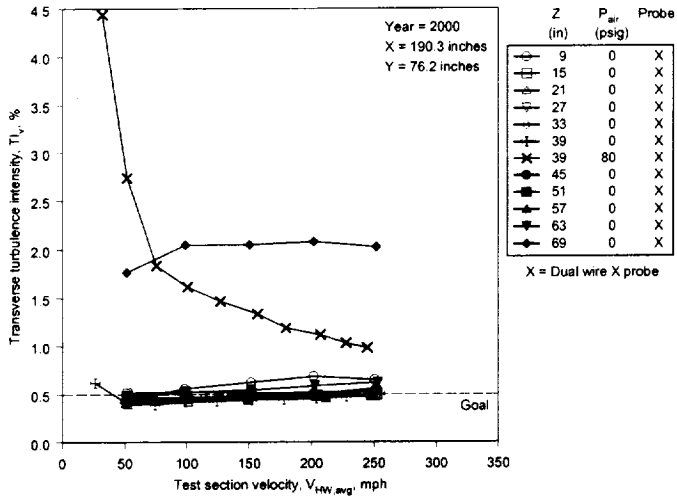


Figure 21.—Hot wire turbulence intensity data for Y=76.2 inches and for the years and parameters as follows: (a) 1997, axial turbulence intensity, (b) 2000, axial turbulence intensity, and (c) 2000, transverse turbulence intensity.

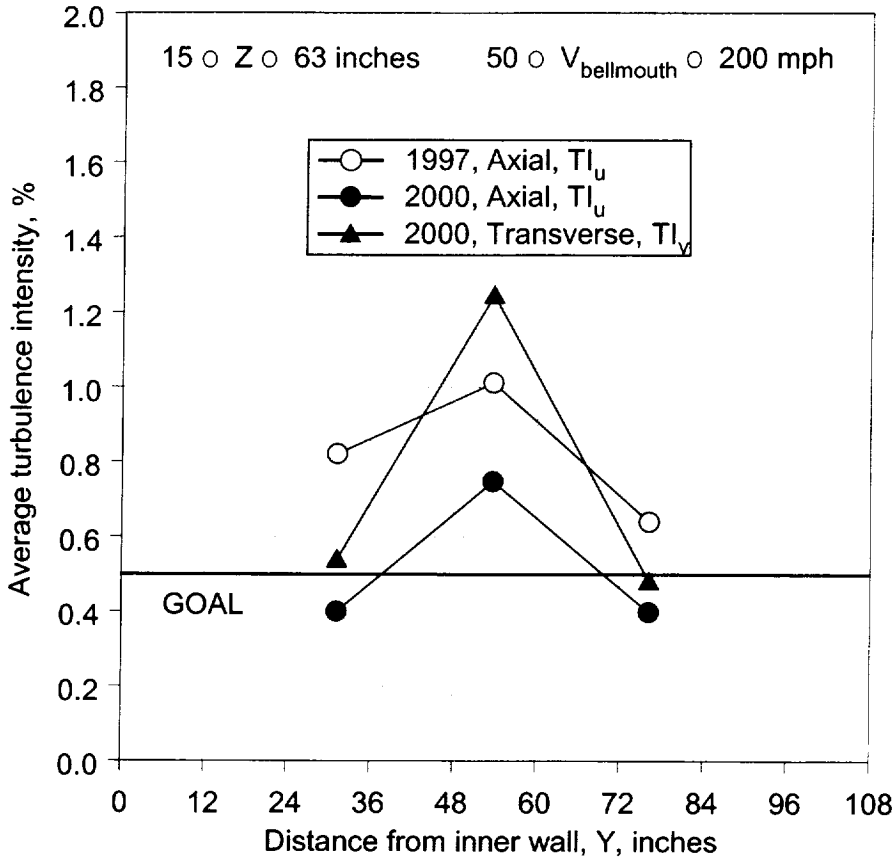


Figure 22.—Average axial and transverse turbulence intensity for the years 1997 and 2000.

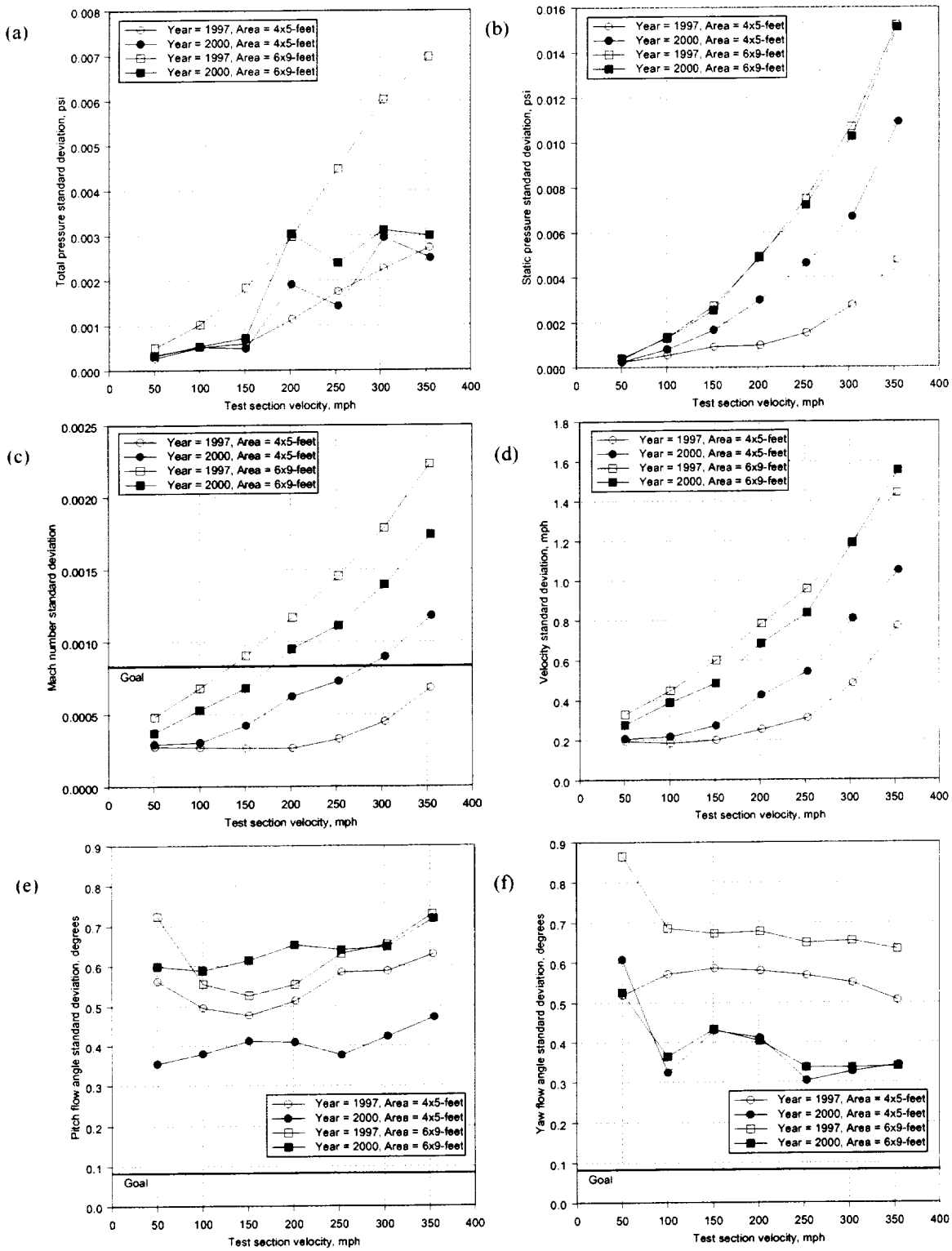


Figure 23.—IRT test section standard deviations for (a) total pressure, (b) static pressure, (c) Mach number, (d) velocity, (e) pitch flow angle, and (f) yaw flow angle, for the years 1997 and 2000, and for the 6x9 and 4x5-foot cross-sectional areas.

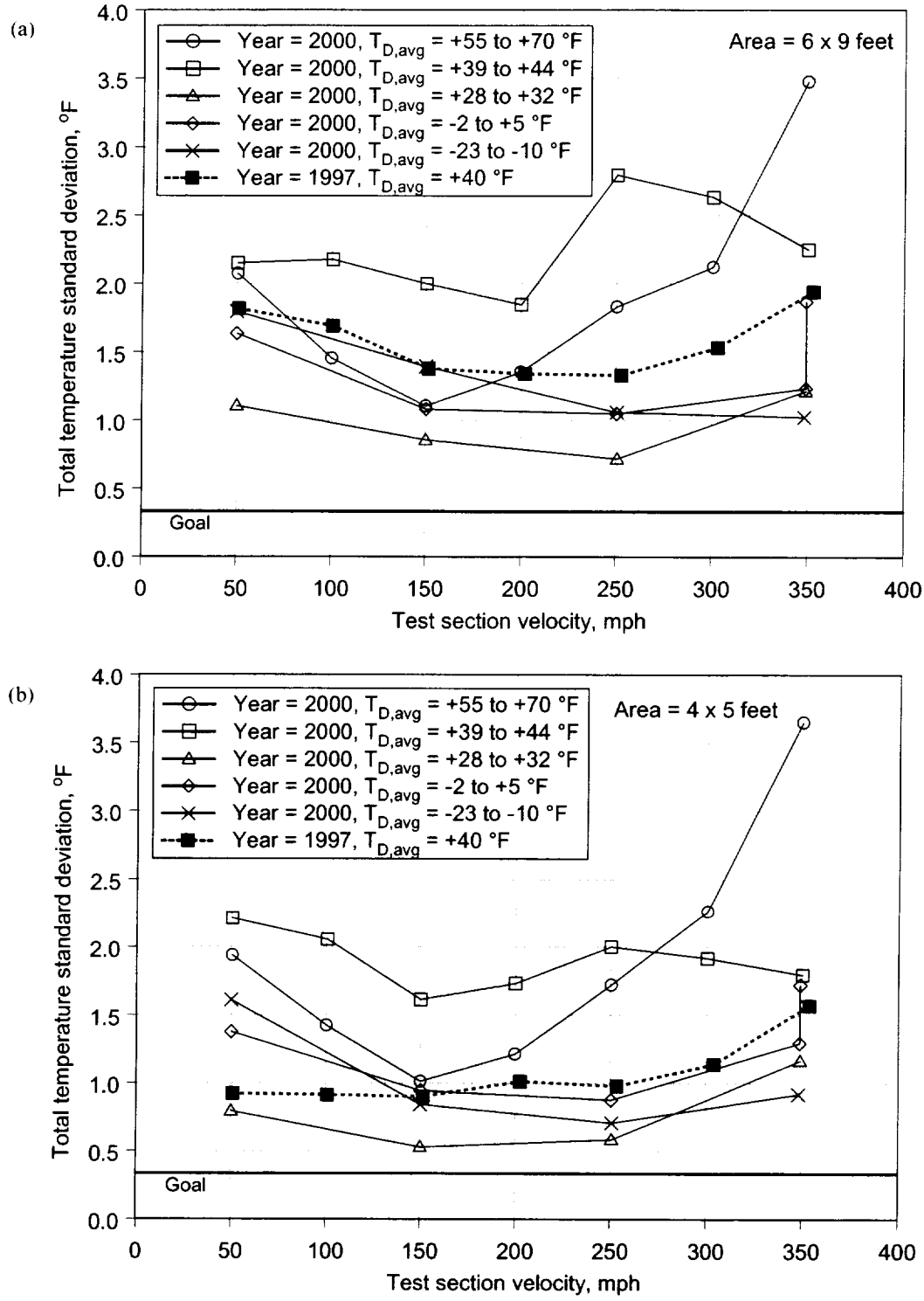


Figure 24.—Total temperature standard deviation for the test section (a) 6x9-foot and (b) 4x5-foot cross-sectional areas, for various total temperatures, and for the years 1997 and 2000.

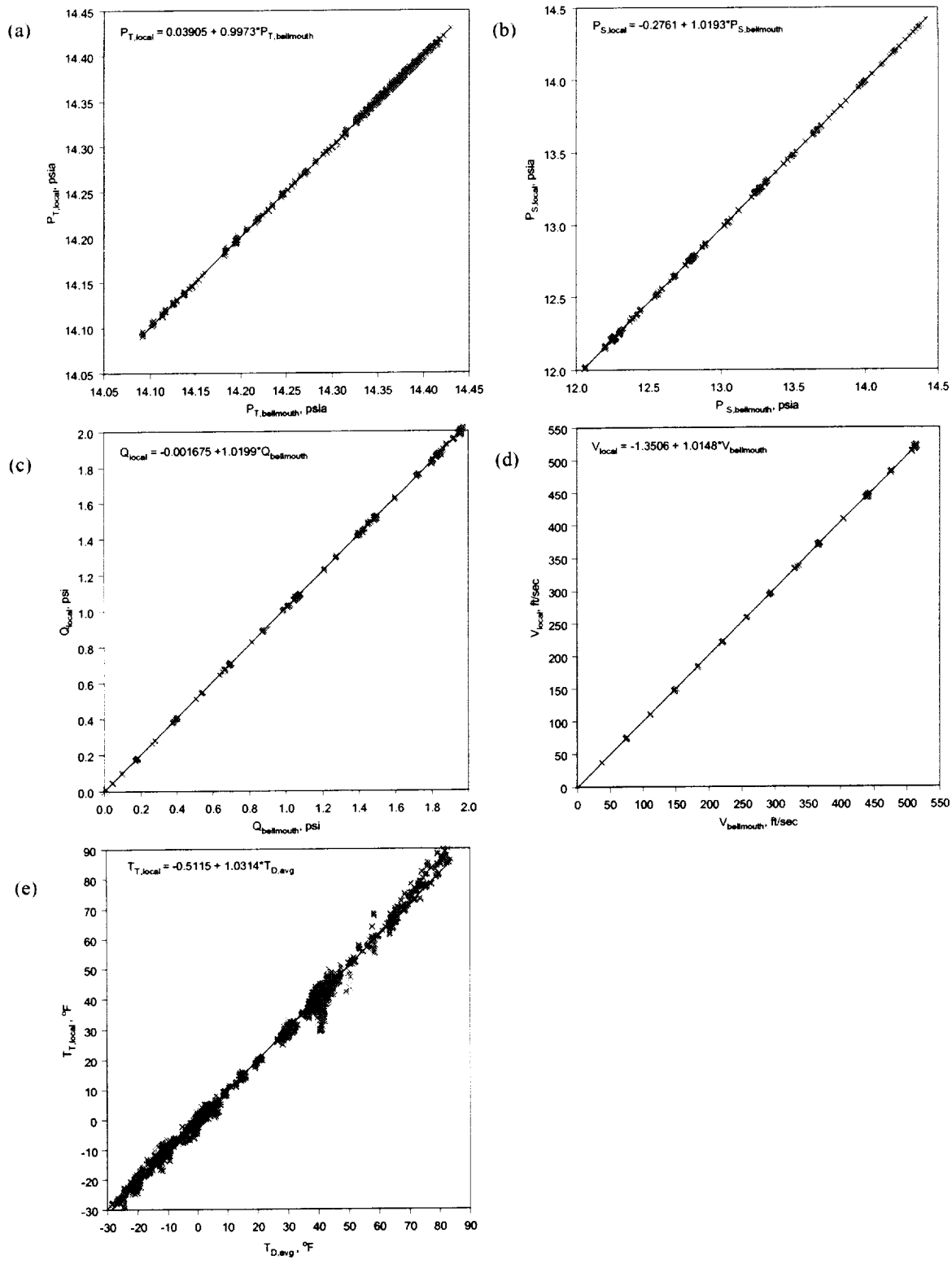


Figure 25.—IRT test section calibration curves for (a) total pressure, (b) static pressure, (c) dynamic pressure, (d) velocity, and (e) total temperature.

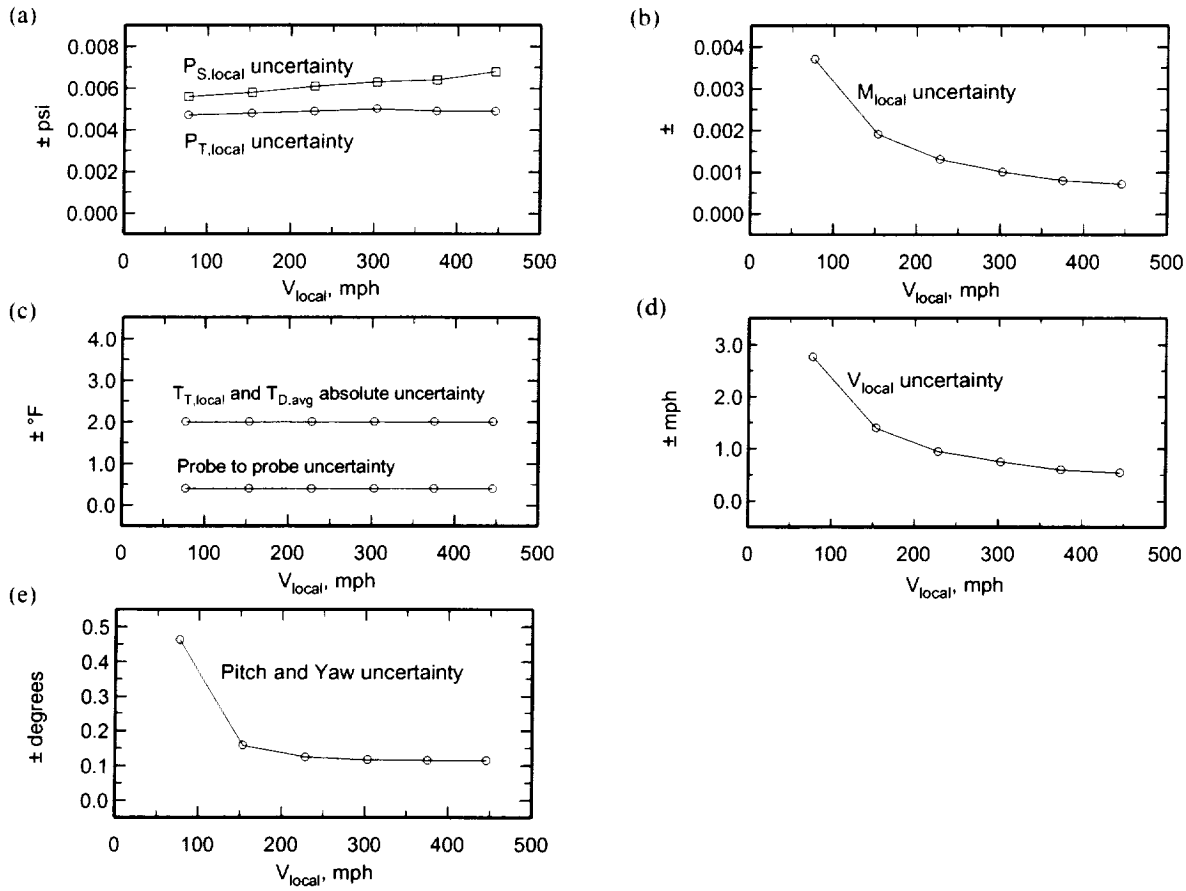


Figure 26.—Measurement uncertainties for (a) total and static pressure, (b) Mach number, (c) total temperature, (d) velocity, and (e) pitch and yaw flow angle.

# REPORT DOCUMENTATION PAGE

*Form Approved*
*OMB No. 0704-0188*



| 1. AGENCY USE ONLY (*Leave blank*) | 2. REPORT DATE | 3. REPORT TYPE AND DATES COVERED |
|---|---|---|
| | March 2001 | Final Contractor Report |

**4. TITLE AND SUBTITLE**

Aero-Thermal Calibration of the NASA Glenn Icing Research Tunnel (2000 Tests)

**5. FUNDING NUMBERS**

WU–708–90–1A–00
NAS3–98008

**6. AUTHOR(S)**

Jose C. Gonsalez, E. Allen Arrington, and Monroe R. Curry III

**7. PERFORMING ORGANIZATION NAME(S) AND ADDRESS(ES)**

Dynacs Engineering Company, Inc.
2001 Aerospace Parkway
Brook Park, Ohio 44142

**8. PERFORMING ORGANIZATION REPORT NUMBER**

E–12612

**9. SPONSORING/MONITORING AGENCY NAME(S) AND ADDRESS(ES)**

National Aeronautics and Space Administration
Washington, DC 20546–0001

**10. SPONSORING/MONITORING AGENCY REPORT NUMBER**

NASA CR—2001-210685
AIAA–2001–0233

**11. SUPPLEMENTARY NOTES**

Prepared for the 39th Aerospace Sciences Meeting and Exhibit sponsored by the American Institute of Aeronautics and Astronautics, Reno, Nevada, January 8–11, 2001. Project Manager, Tom Burke, Resources Analysis and Management Office, NASA Glenn Research Center, organization code 0210, 216–433–5172.

**12a. DISTRIBUTION/AVAILABILITY STATEMENT**

Unclassified - Unlimited
Subject Category: 09 Distribution: Nonstandard

Available electronically at http://gltrs.grc.nasa.gov/GLTRS

This publication is available from the NASA Center for AeroSpace Information, 301–621–0390.

**12b. DISTRIBUTION CODE**

**13. ABSTRACT** ***(Maximum 200 words)***

Aerothermal calibration measurements and flow quality surveys were made in the test section of the Icing Research Tunnel at the NASA Glenn Research Center. These surveys were made following major facility modifications including widening of the heat exchanger tunnel section, replacement of the heat exchanger, installation of new turning vanes, and installation of new fan exit guide vanes. Standard practice at NASA Glenn requires that test section calibration and flow quality surveys be performed following such major facility modifications. A single horizontally oriented rake was used to survey the flow field at several vertical positions within a single cross-sectional plane of the test section. These surveys provided a detailed mapping of the total and static pressure, total temperature, Mach number, velocity, flow angle and turbulence intensity. Data were acquired over the entire velocity and total temperature range of the facility. No icing conditions were tested; however, the effects of air sprayed through the water injecting spray bars were assessed. All data indicate good flow quality. Mach number standard deviations were less than 0.0017, flow angle standard deviations were between 0.3° and 0.8°, total temperature standard deviations were between 0.5 and 1.8 °F for subfreezing conditions, axial turbulence intensities varied between 0.3 and 1.0 percent, and transverse turbulence intensities varied between 0.3 and 1.5 percent. Measurement uncertainties were also quantified.

**14. SUBJECT TERMS**

Wind tunnel; Calibration; Flow quality; Subsonic; Icing

**15. NUMBER OF PAGES**

45

**16. PRICE CODE**

A03

| 17. SECURITY CLASSIFICATION OF REPORT | 18. SECURITY CLASSIFICATION OF THIS PAGE | 19. SECURITY CLASSIFICATION OF ABSTRACT | 20. LIMITATION OF ABSTRACT |
|---|---|---|---|
| Unclassified | Unclassified | Unclassified | |